Main SST-SLP coupled modes in the South Pacific as simulated by IPCC-AR4 coupled models

Aldo Montecinos
Departamento de Geofísica
Universidad de Concepción

II Simposio Internacional de Climatología, Sao Pablo, Brasil, 2-3 noviembre 2007

DGEO
Universidad de Concepción

- **The projected XXI Century climate change in the IPCC - Fourth Assessment Report (AR4) is based on coupled models**

- **The projected XXI Century climate change in the IPCC - Fourth Assessment Report (AR4) is based on coupled models**

- **El Niño-Southern Oscillation (ENSO) is one of the most important sources of interannual variability in the climate system… (also at interdecadal timescale)**

- **The projected XXI Century climate change in the IPCC - Fourth Assessment Report (AR4) is based on coupled models**

- **El Niño-Southern Oscillation (ENSO) is one of the most important sources of interannual variability in the climate system… (also at interdecadal timescale)**

- **ENSO must be simulated properly by coupled models**

1. AchutaRao, Krishna and K. R. Sperber, 2006: ENSO Simulation in Coupled Ocean-Atmosphere Models: Are the Current Models Better?. *Climate Dynamics*, 10.1007/s00382-006-0119-7.
2. Annamalai, H., K. Hamilton, and K. R. Sperber, South Asian summer monsoon and its relationship with ENSO in the IPCC AR4 simulations. *J. Climate*. Submitted.
3. Capotondi, A., A. T. Wittenberg, and S. Masina, 2006: Spatial and temporal structure of tropical Pacific interannual variability in 20th century coupled simulations. *Ocean Modeling*. In press.
4. Guilyardi, E., 2006: El Niño – mean state – seasonal cycle interactions in a multi–model ensemble. *Clim Dyn*, **26**, 329-348, DOI:10.1007/s00382-005-0084-6.
5. Joseph, R., and S. Nigam, 2006: ENSO Evolution and Teleconnections in IPCC's 20th Century Climate Simulations: Realistic Representation?. *J. Climate*. Accepted.
6. Merryfield, W.J., 2006: Changes to ENSO under CO2 doubling in a multi-model ensemble. *J. Climate*, **19**, 4009-4027, DOI: 10.1175/JCLI3834.1.
7. Philip, S.Y., and G.J. Van Oldenborgh, 2006: Shifts in ENSO coupling processes under global warming. *GRL*, **33**, L11704, doi:10.1029/2006GL026196.
8. Phillips, T.J., and P.J. Gleckler, 2006: Evaluation of continental precipitation in 20th century climate simulations: The utility of multimodel statistics. *Water Resources Research*, **42**, 10.1029/2005WR004313. In press.
9. Sang-Wook Yeh and B. P. Kirtman, 2007: ENSO amplitude changes due to climate change projections in different coupled models. *Journal of climate*, **20**, 203-217.
10. Sang-Wook Yeh, Young-Gyu Park and Ben P. Kirtman, 2006: ENSO amplitude changes in climate change commitment to. *Geophy. Res. Lett.*. Accepted.
11. Van Oldenborgh, G.J., and S.Y. Philip, and M. Collins, 2005: El Niño in a changing climate: a multi-model study.. *Ocean Science*, **1**, 81-95, SREF:1812-0792/os/2005-1-81.
12. Yamaguchi, K., and A. Noda, 2006: Global Warming Patterns over the North Pacific: ENSO versus AO. *J. Meteor. Soc. Japan*, **84**, 221-241, doi:10.2151/jmsj.84.221.
13. Zhang, T., and D.-Z. Sun, 2006: Response of water vapor and clouds to El Niño warming in three National Center for Atmospheric Research atmospheric models. *J. Geophys. Res.*, **111**, D17103, doi:10.1029/2005JD006700.

1. AchutaRao, Krishna and K. R. Sperber, 2006: ENSO Simulation in Coupled Ocean-Atmosphere Models: Are the Current Models Better?. *Climate Dynamics*, 10.1007/s00382-006-0119-7.
2. Annamalai, H., K. Hamilton, and K. R. Sperber, South Asian summer monsoon and its relationship with ENSO in the IPCC AR4 simulations. *J. Climate*. Submitted.
3. Capotondi, A., A. T. Wittenberg, and S. Masina, 2006: Spatial and temporal structure of tropical Pacific interannual variability in 20th century coupled simulations. *Ocean Modeling*. In press.
4. Guilyardi, E., 2006: El Niño – mean state – seasonal cycle interactions in a multi–model ensemble. *Clim Dyn*, **26**, 329-348, DOI:10.1007/s00382-005-0084-6.
5. Joseph, R., and S. Nigam, 2006: ENSO Evolution and Teleconnections in IPCC's 20th Century Climate Simulations: Realistic Representation?. *J. Climate*. Accepted.
6. Merryfield, W.J., 2006: Changes to ENSO under CO2 doubling in a multi-model ensemble. *J. Climate*, **19**, 4009-4027, DOI: 10.1175/JCLI3834.1.
7. Philip, S.Y., and G.J. Van Oldenborgh, 2006: Shifts in ENSO coupling processes under global warming. *GRL*, **33**, L11704, doi:10.1029/2006GL026196.
8. Phillips, T.J., and P.J. Gleckler, 2006: Evaluation of continental precipitation in 20th century climate simulations: The utility of multimodel statistics. *Water Resources Research*, **42**, 10.1029/2005WR004313. In press.
9. Sang-Wook Yeh and B. P. Kirtman, 2007: ENSO amplitude changes due to climate change projections in different coupled models. *Journal of climate*, **20**, 203-217.
10. Sang-Wook Yeh, Young-Gyu Park and Ben P. Kirtman, 2006: ENSO amplitude changes in climate change commitment to. *Geophy. Res. Lett.*. Accepted.
11. Van Oldenborgh, G.J., and S.Y. Philip, and M. Collins, 2005: El Niño in a changing climate: a multi-model study.. *Ocean Science*, **1**, 81-95, SREF:1812-0792/os/2005-1-81.
12. Yamaguchi, K., and A. Noda, 2006: Global Warming Patterns over the North Pacific: ENSO versus AO. *J. Meteor. Soc. Japan*, **84**, 221-241, doi:10.2151/jmsj.84.221.
13. Zhang, T., and D.-Z. Sun, 2006: Response of water vapor and clouds to El Niño warming in three National Center for Atmospheric Research atmospheric models. *J. Geophys. Res.*, **111**, D17103, doi:10.1029/2005JD006700.

• ENSO (or El Niño) has been diagnosed using SST anomalies or the Niño 3 (Niño 3.4) SST amplitudes…

Van Oldenborgh, G.J., and S.Y. Philip, and M. Collins, 2005

First EOF of detrended SST
in the region 10°S–10 °N, 120°E–90°W

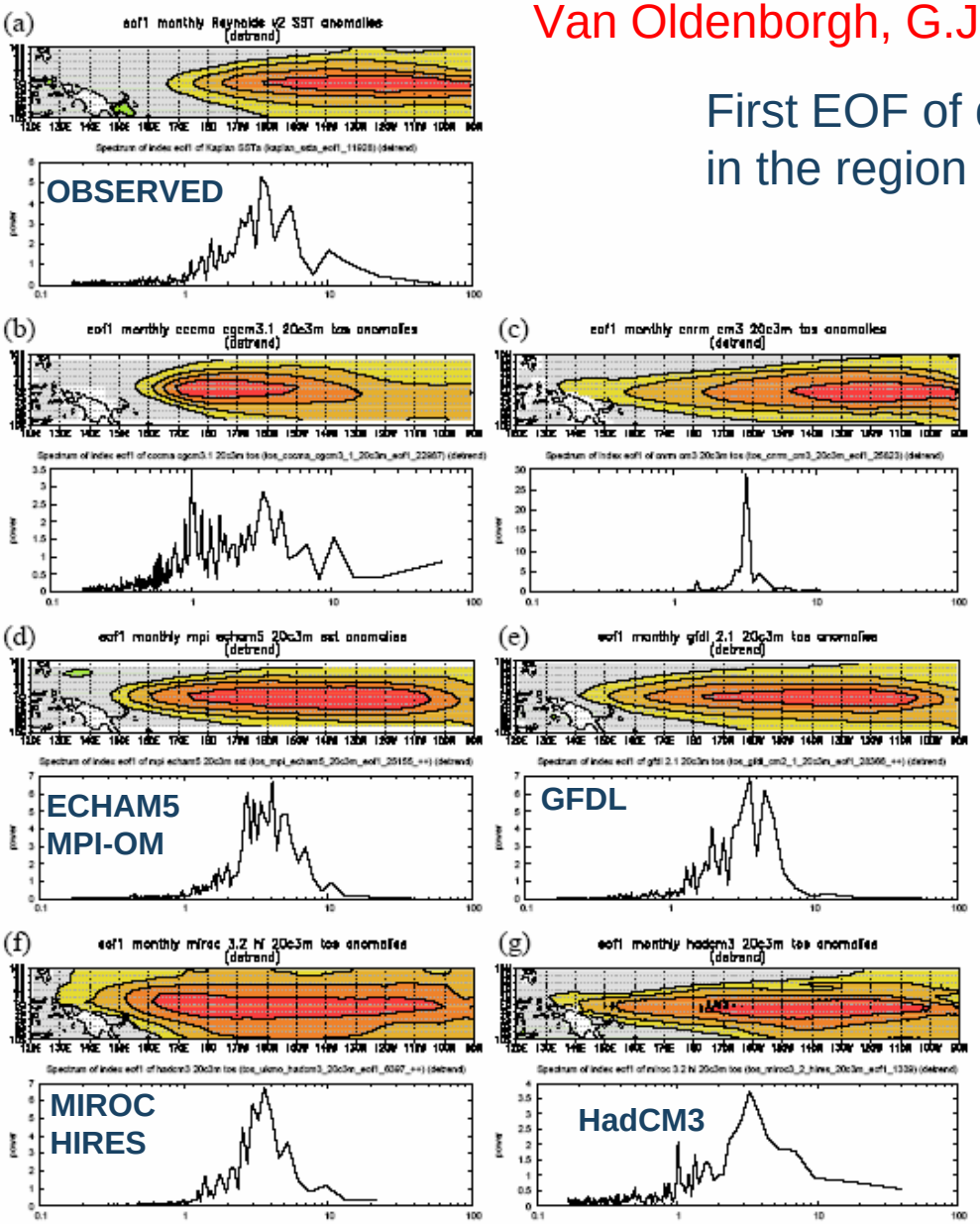

Fig. 2. Examples of the first EOF of detrended SST in the region 10° S–10° N, 120° E–90° W and the spectrum of its corresponding time series. The pattern is normalized to have unit amplitude and the contour interval is 0.2. (a) Observations: the pattern of SSTOIv2 and the time series of Kaplan SST, (b) CGCM3.1(T47), (c) CNRM-CM3, (d) ECHAM5/MPI-OM, (e) GFDL-CM2.1, (f) MIROC3.2(hires) and (g) HadCM3.

Van Oldenborgh, G.J., and S.Y. Philip, and M. Collins, 2005

First EOF of detrended SST
in the region 10°S–10 °N, 120°E–90°W

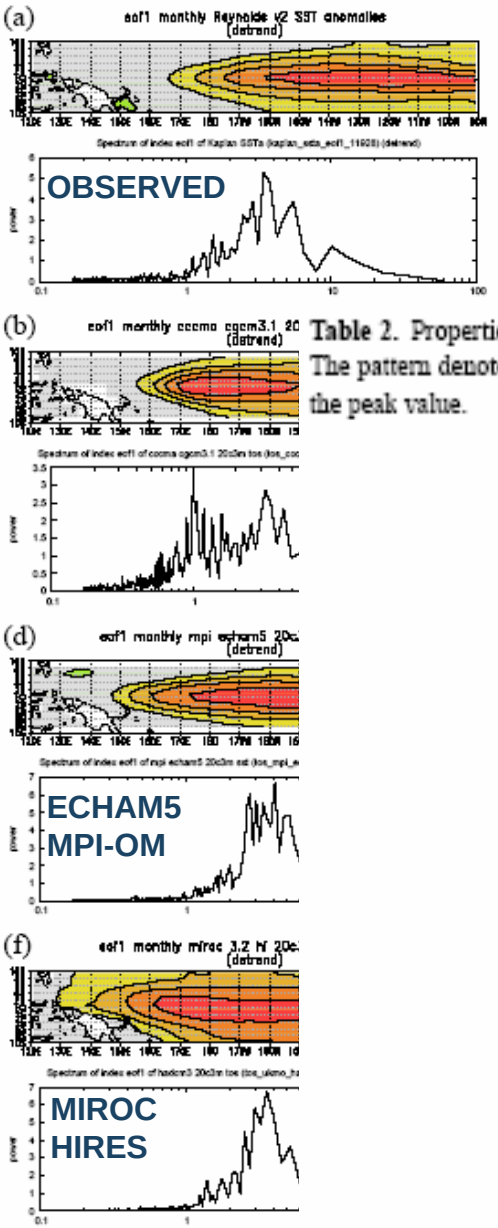

Table 2. Properties of the first EOF and associated time series (PC) of detrended monthly SST in the region 10° S–10° N, 120° E–90° W. The pattern denotes the longitudes of the contour of 80% of the peak value, the period denotes the height of the power spectrum at 50% of the peak value.

Analysis/model	Pattern	Period (yr)	Amplitude	Skewness
SSTOIv2/Kaplan	160° W–<90° W	2.5–6	0.25	0.54
CCSM3	160° W–100° W	2–2.5	0.22	−0.06
CGCM3.1(T47)	170° E–150° W	2.5–5	0.14	0.08
CNRM-CM3	160° W–<90° W	3.1–3.5	0.48	−0.13
CSIRO-Mk3.0	160° E–95° W	2–4	0.27	0.04
ECHAM5/MPI-OM	175° W–105° W	2.5–7	0.47	0.08
FGOALS-g1.0	180°–105° W	3.0–3.3	0.57	−0.18
GFDL-CM2.0	175° E–115° W	1.5–3.5	0.32	0.14
GFDL-CM2.1	180°–105° W	2–6	0.39	0.31
GISS-AOM	140° E–<90° W	1–10	0.09	−0.01
GISS-EH	150° W–100° W	1.5–4	0.16	−0.20
GISS-ER	170° W–<90° W	2.5–8	0.07	−0.18
INM-CM3.0	150° E–155° W	1.5–9	0.34	0.42
IPSL-CM4	175° W–100° W	2.2–2.7	0.28	−0.12
MIROC3.2(hires)	160° E–100° W	2.5–7	0.17	0.63
MIROC3.2(medres)	155° E–105° W	3–10	0.25	0.16
MRI-CGCM2.3.2	180°–105° W	1.8–3.5	0.26	0.55
PCM	145° W–100° W	1.5–5	0.23	0.21
UKMO-HadCM3	175° W–100° W	2.5–5	0.32	0.21
UKMO-HadGEM1	145° W–110° W	4.1–4.4	0.17	0.15

Fig. 2. Examples of the first EOF of detre
series. The pattern is normalized to have u
time series of Kaplan SST, (b) CGCM3.1(T47), (c) CNRM-CM3, (d) ECHAM5/MPI-OM, (e) GFDL-CM2.1, (f) MIROC3.2(hires) and (g) HadCM3.

Van Oldenborgh, G.J., and S.Y. Philip, and M. Collins, 2005

First EOF of detrended SST
in the region 10°S–10 °N, 120°E–90°W

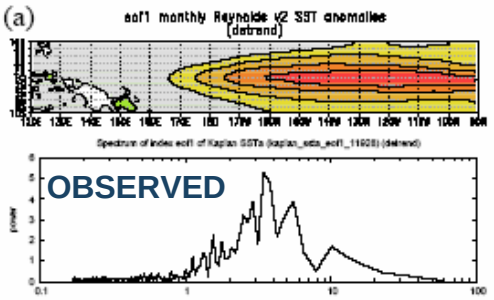

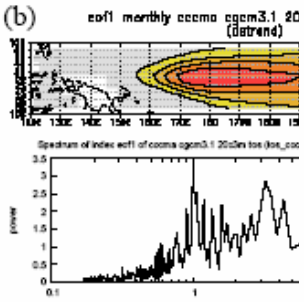

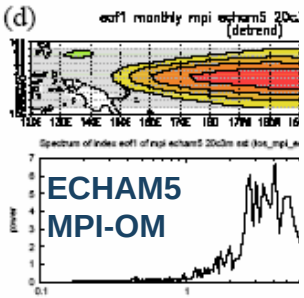

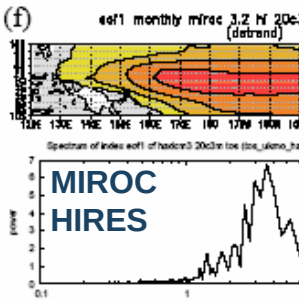

Fig. 2. Examples of the first EOF of detre
series. The pattern is normalized to have u
time series of Kaplan SST, (b) CGCM3.1(T47), (c) CNRM-CM3, (d) ECHAM5/MPI-OM, (e) GFDL-CM2.1, (f) MIROC3.2(hires) and (g) HadCM3.

Table 2. Properties of the first EOF and associated time series (PC) of detrended monthly SST in the region 10° S–10° N, 120° E–90° W. The pattern denotes the longitudes of the contour of 80% of the peak value, the period denotes the height of the power spectrum at 50% of the peak value.

Analysis/model	Pattern	Period (yr)	Amplitude	Skewness
SSTOIv2/Kaplan	160° W–<90° W	2.5–6	0.25	0.54
CCSM3	160° W–100° W	2–2.5	0.22	−0.06
CGCM3.1(T47)	170° E–150° W	2.5–5	0.14	0.08
CNRM-CM3	160° W–<90° W	3.1–3.5	0.48	−0.13
CSIRO-Mk3.0	160° E–95° W	2–4	0.27	0.04
ECHAM5/MPI-OM	175° W–105° W	2.5–7	0.47	0.08
FGOALS-g1.0	180°–105° W	3.0–3.3	0.57	−0.18
GFDL-CM2.0	175° E–115° W	1.5–3.5	0.32	0.14
GFDL-CM2.1	180°–105° W	2–6	0.39	0.31
GISS-AOM	140° E–<90° W	1–10	0.09	−0.01
GISS-EH	150° W–100° W	1.5–4	0.16	−0.20
GISS-ER	170° W–<90° W	2.5–8	0.07	−0.18
INM-CM3.0	150° E–155° W	1.5–9	0.34	0.42
IPSL-CM4	175° W–100° W	2.2–2.7	0.28	−0.12
MIROC3.2(hires)	160° E–100° W	2.5–7	0.17	0.63
MIROC3.2(medres)	155° E–105° W	3–10	0.25	0.16
MRI-CGCM2.3.2	180°–105° W	1.8–3.5	0.26	0.55
PCM	145° W–100° W	1.5–5	0.23	0.21
UKMO-HadCM3	175° W–100° W	2.5–5	0.32	0.21
UKMO-HadGEM1	145° W–110° W	4.1–4.4	0.17	0.15

Guilyardi, E., 2006

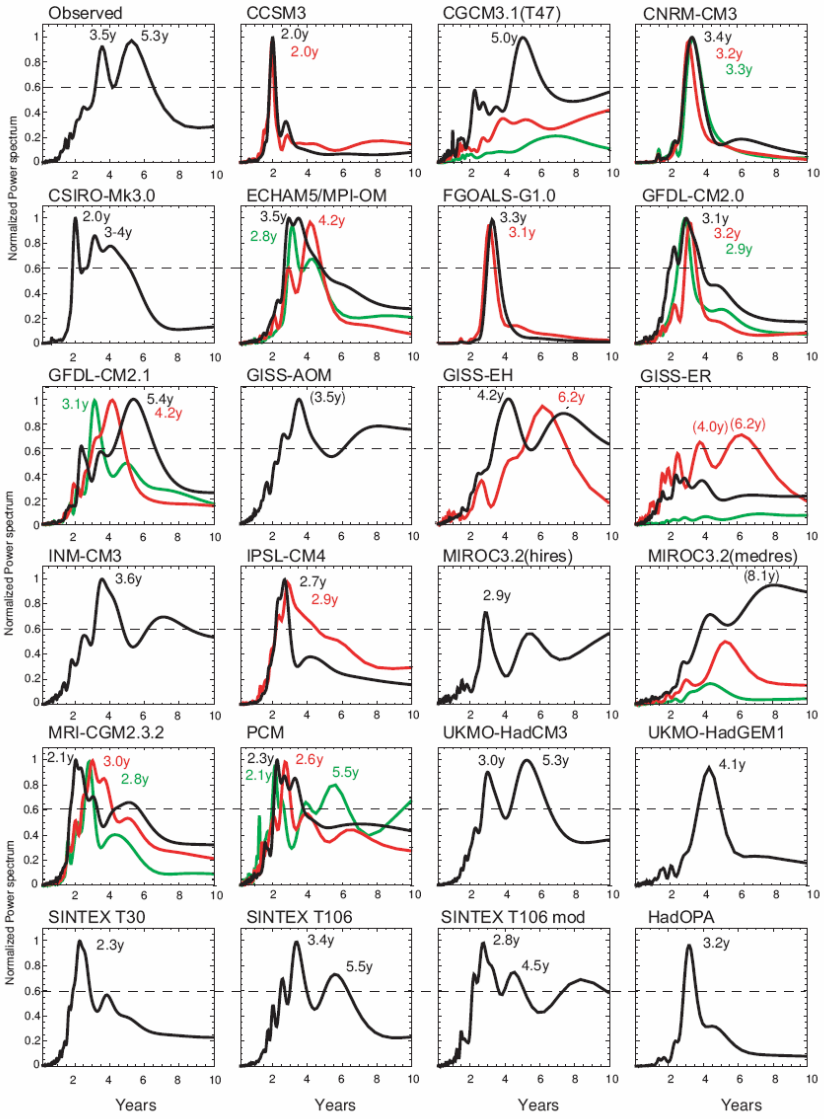

Figure 1: Normalized power spectra of Niño3 SSTA for the 23 models studied, together with the available scenarios. Observation are for the HadISST1.1 dataset, years 1900-2000. Models color code: black = picntrl, red = 1pctto2x (after stabilisation), green = 1pctto4x (after stabilisation). Spectral peaks exceeding 0.6 are significant.

Amplitude of El Niño is defined as the monthly standard deviation of the SST anomaly in the Niño 3 region

Guilyardi, E., 2006

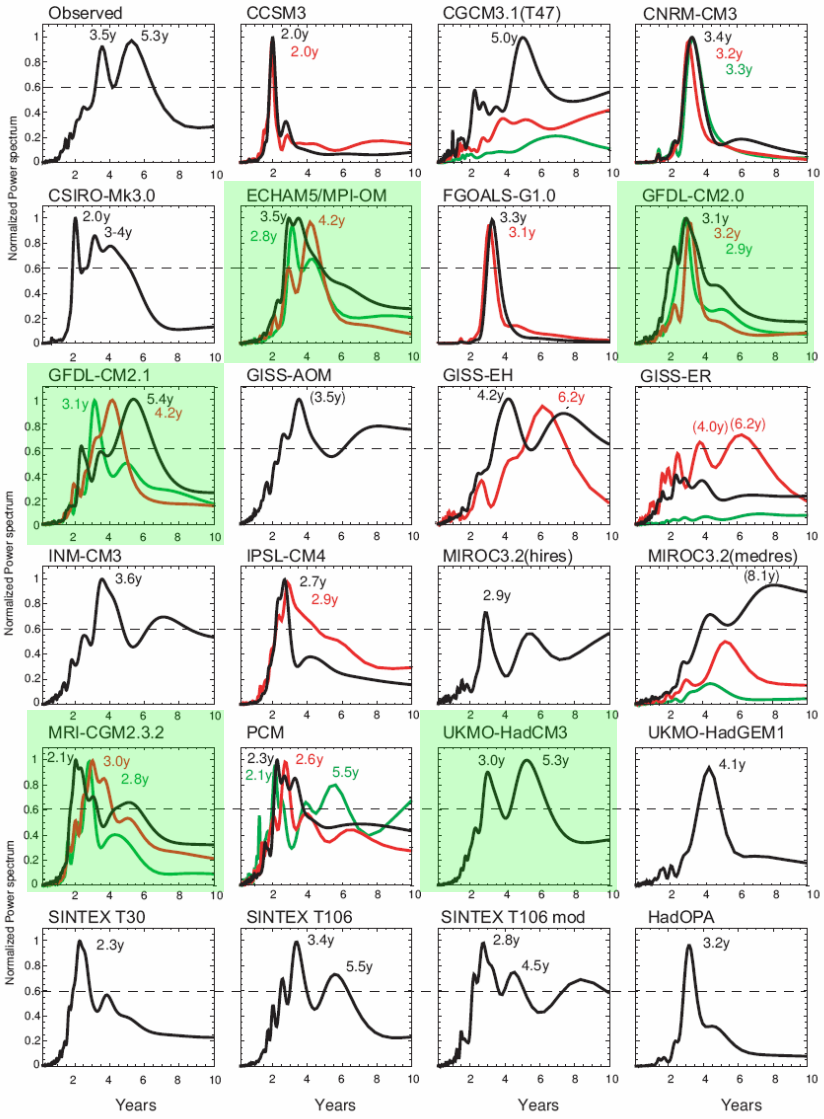

Amplitude of El Niño is defined as the monthly standard deviation of the SST anomaly in the Niño 3 region

These models also best simulate the Tropical Pacific climatology…

Figure 1: Normalized power spectra of Niño3 SSTA for the 23 models studied, together with the available scenarios. Observation are for the HadISST1.1 dataset, years 1900-2000. Models color code: black = picntrl, red = 1pctto2x (after stabilisation), green = 1pctto4x (after stabilisation). Spectral peaks exceeding 0.6 are significant.

Joseph, R., and S. Nigam, 2006

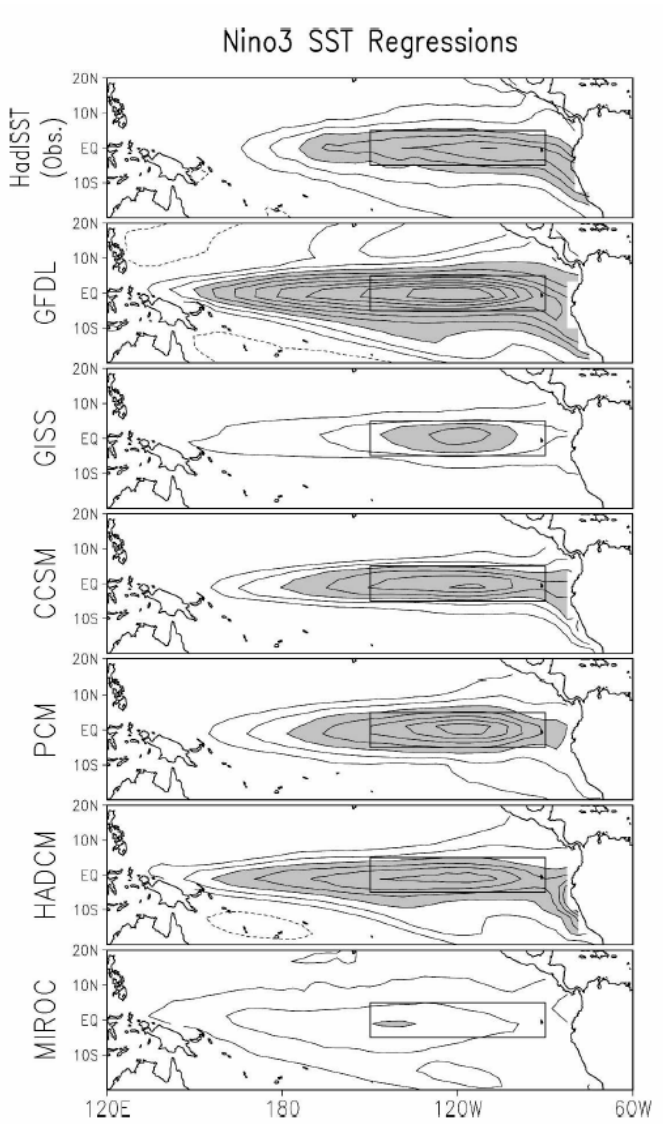

FIG. 1. Niño-3 SST index regressions on observed and simulated SSTs in the 1950–99 period, based on all calendar month anomalies. The marked rectangular box outlines the Niño-3 region (5°S–5°N, 150°–90°W). SST observations are from the HadISST analysis. Simulating models are noted at the left of each panel. The contour interval is 0.2 K and the zero contour is suppressed; the shading threshold is 0.6 K.

Joseph, R., and S. Nigam, 2006

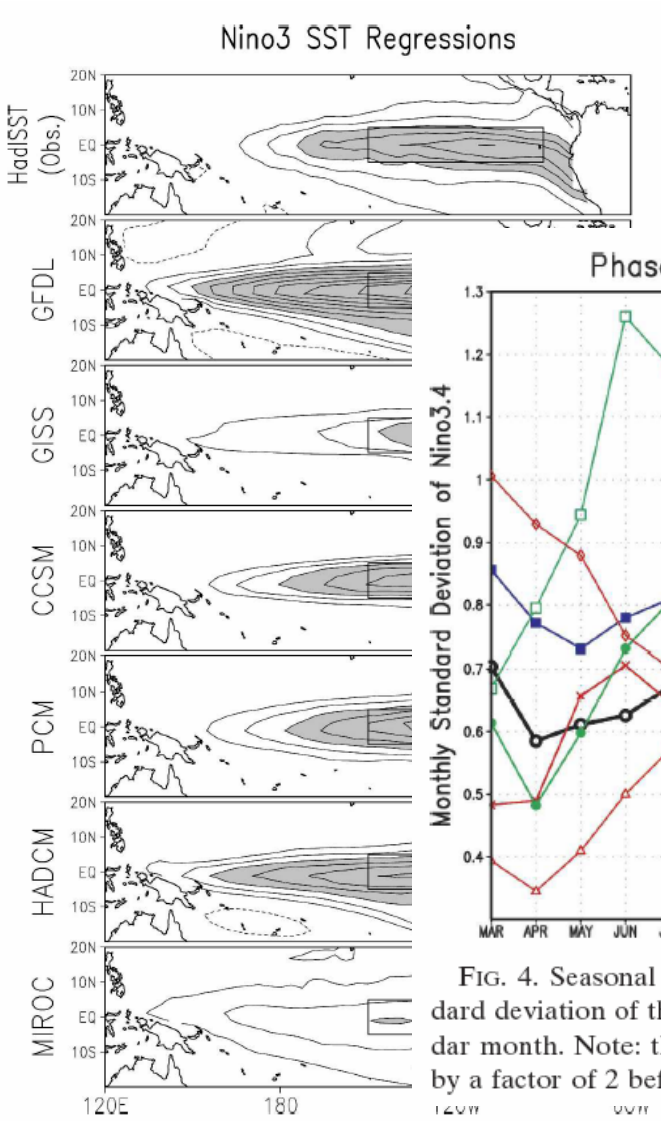

FIG. 1. Niño-3 SST index regressions on observed and simulated SSTs in the 1950–99 period, based on all calendar month anomalies. The marked rectangular box outlines the Niño-3 region (5°S–5°N, 150°–90°W). SST observations are from the HadISST analysis. Simulating models are noted at the left of each panel. The contour interval is 0.2 K and the zero contour is suppressed; the shading threshold is 0.6 K.

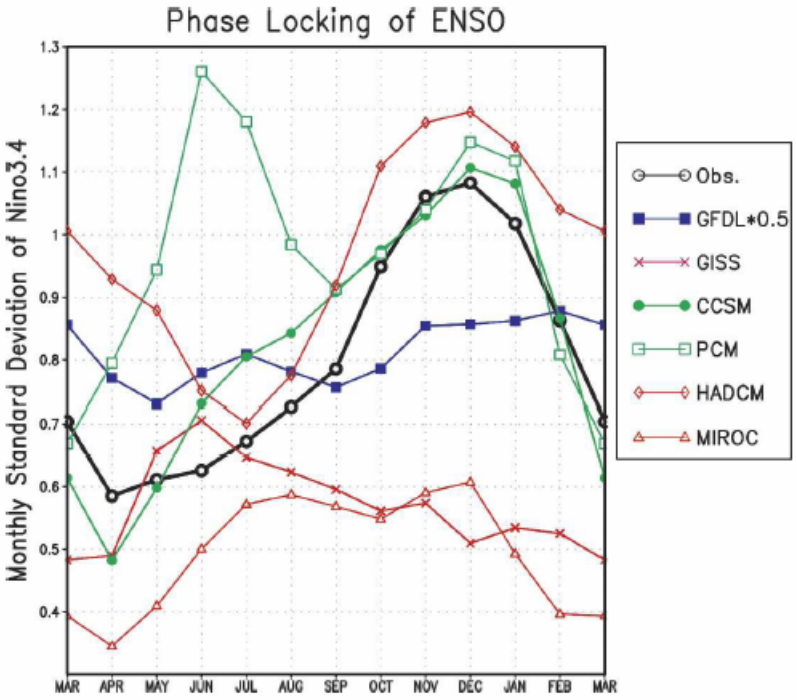

FIG. 4. Seasonal phase-locking of ENSO variability: the standard deviation of the Niño-3.4 SST index is shown in each calendar month. Note: the GFDL values have been scaled downward by a factor of 2 before display.

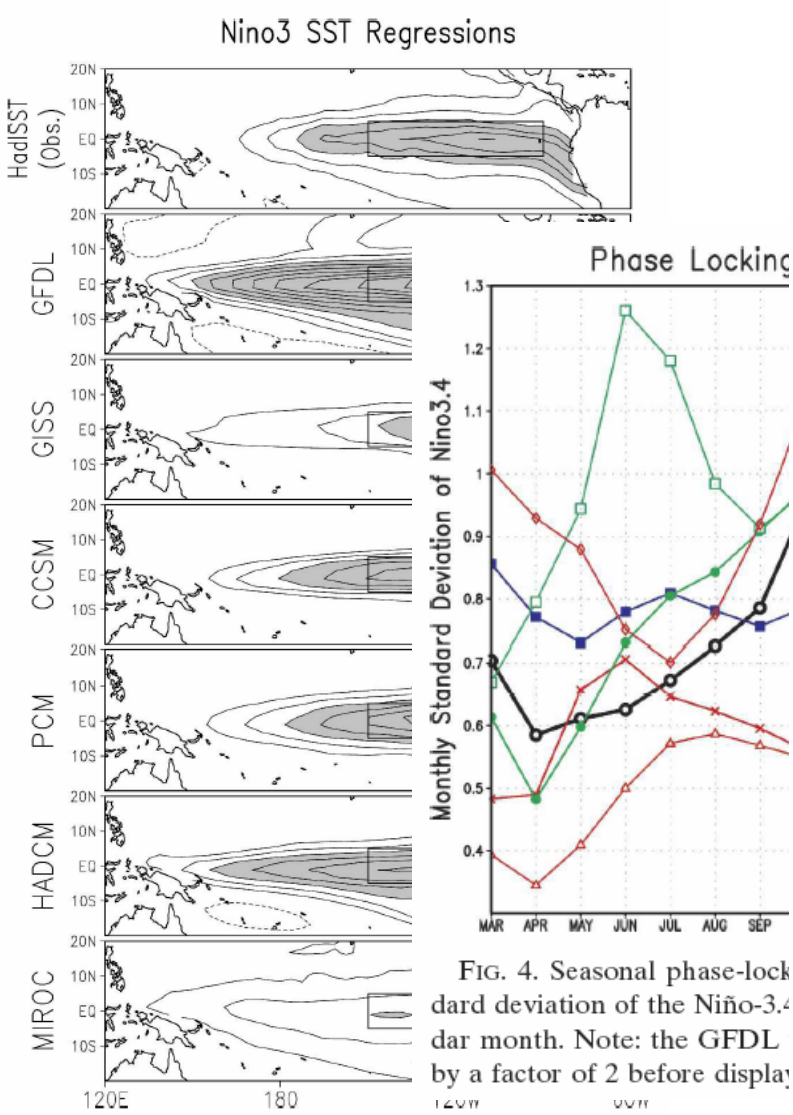

FIG. 1. Niño-3 SST index regressions on observed and simulated SSTs in the 1950–99 period, based on all calendar month anomalies. The marked rectangular box outlines the Niño-3 region (5°S–5°N, 150°–90°W). SST observations are from the HadISST analysis. Simulating models are noted at the left of each panel. The contour interval is 0.2 K and the zero contour is suppressed; the shading threshold is 0.6 K.

FIG. 4. Seasonal phase-lock
dard deviation of the Niño-3.4
dar month. Note: the GFDL
by a factor of 2 before displa

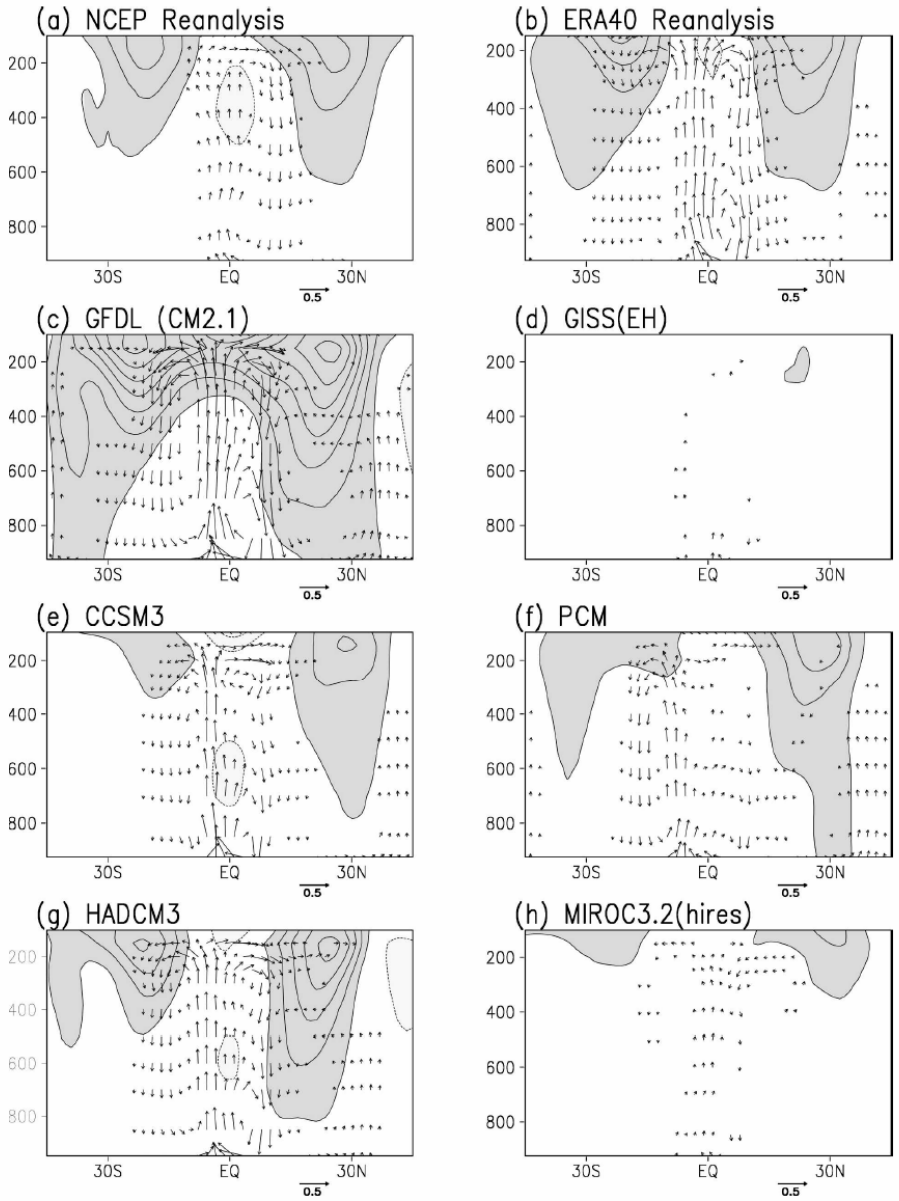

FIG. 8. ENSO's zonally symmetric winter circulation response in the Tropics/subtropics: Niño-3 SST index regressions on zonal-mean zonal wind (rotational flow) are shown using a contour interval and a shading threshold of 0.5 m s^{-1}; the zero contour is omitted in all panels. Regressions on divergent (Hadley) circulation are shown using vectors, whose zonal component denotes zonal-mean meridional wind (in m s^{-1}) and whose vertical component denotes the zonal-mean vertical velocity (in Pa h^{-1}). Vectors of magnitude less than 0.05 are suppressed. The same vector scale, shown below the panels, is used in all cases. Light (dark) shading denotes negative (positive) values.

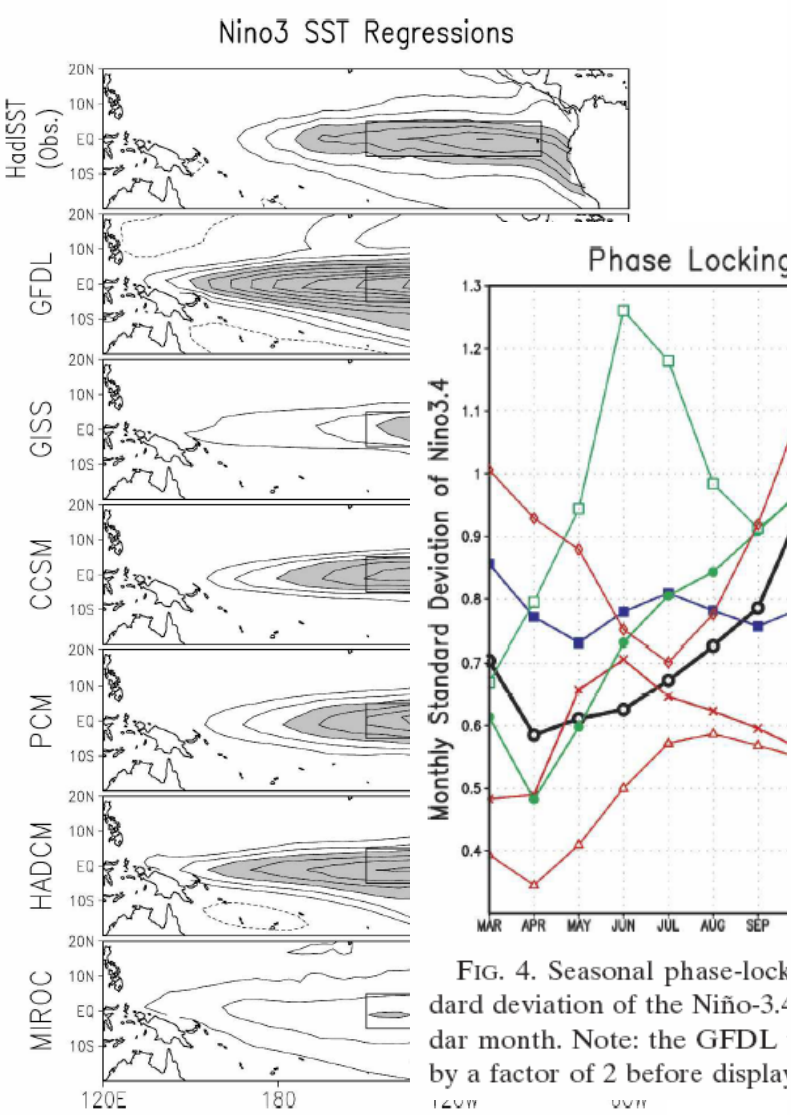

FIG. 1. Niño-3 SST index regressions on observed and simulated SSTs in the 1950–99 period, based on all calendar month anomalies. The marked rectangular box outlines the Niño-3 region (5°S–5°N, 150°–90°W). SST observations are from the HadISST analysis. Simulating models are noted at the left of each panel. The contour interval is 0.2 K and the zero contour is suppressed; the shading threshold is 0.6 K.

FIG. 4. Seasonal phase-lock
dard deviation of the Niño-3.4
dar month. Note: the GFDL
by a factor of 2 before displa

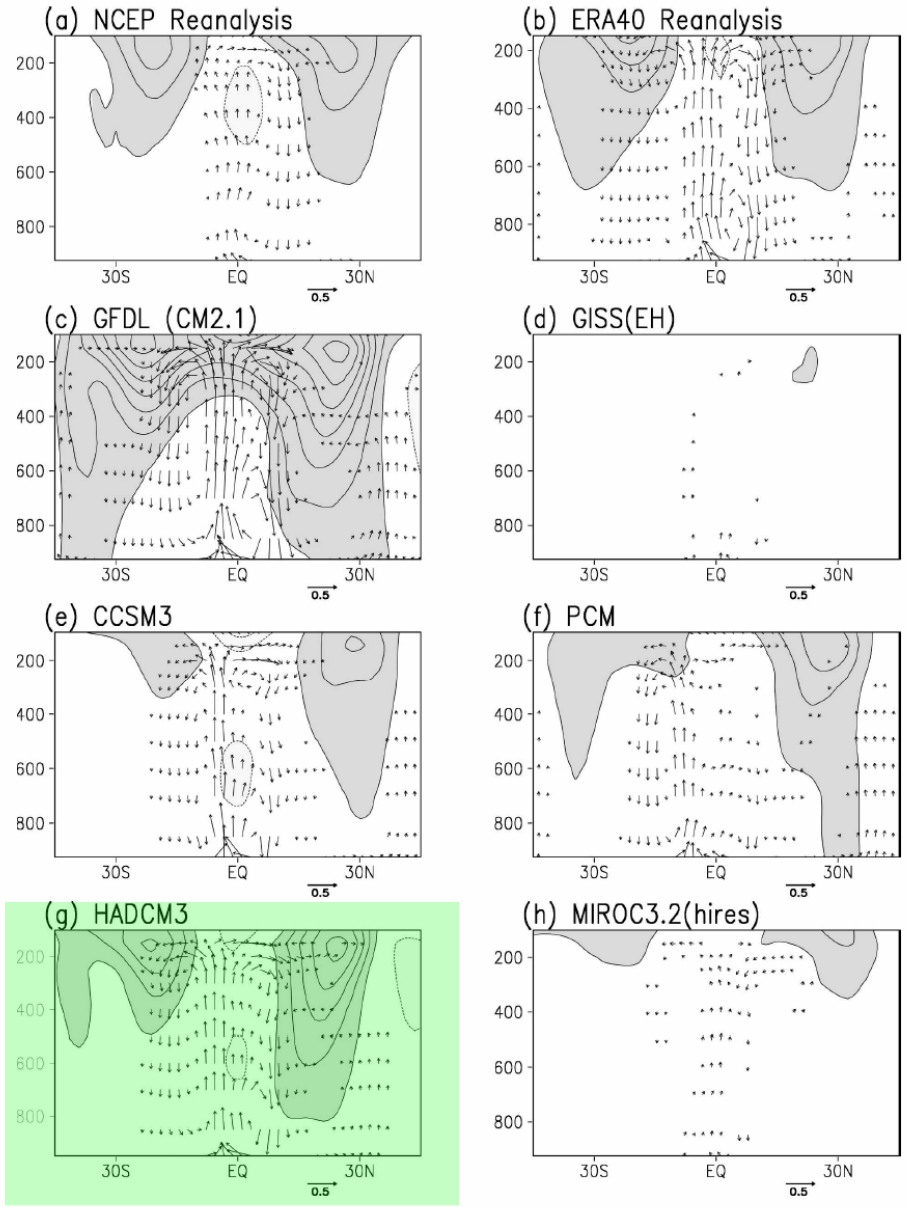

FIG. 8. ENSO's zonally symmetric winter circulation response in the Tropics/subtropics: Niño-3 SST index regressions on zonal-mean zonal wind (rotational flow) are shown using a contour interval and a shading threshold of 0.5 m s^{-1}; the zero contour is omitted in all panels. Regressions on divergent (Hadley) circulation are shown using vectors, whose zonal component denotes zonal-mean meridional wind (in m s^{-1}) and whose vertical component denotes the zonal-mean vertical velocity (in Pa h^{-1}). Vectors of magnitude less than 0.05 are suppressed. The same vector scale, shown below the panels, is used in all cases. Light (dark) shading denotes negative (positive) values.

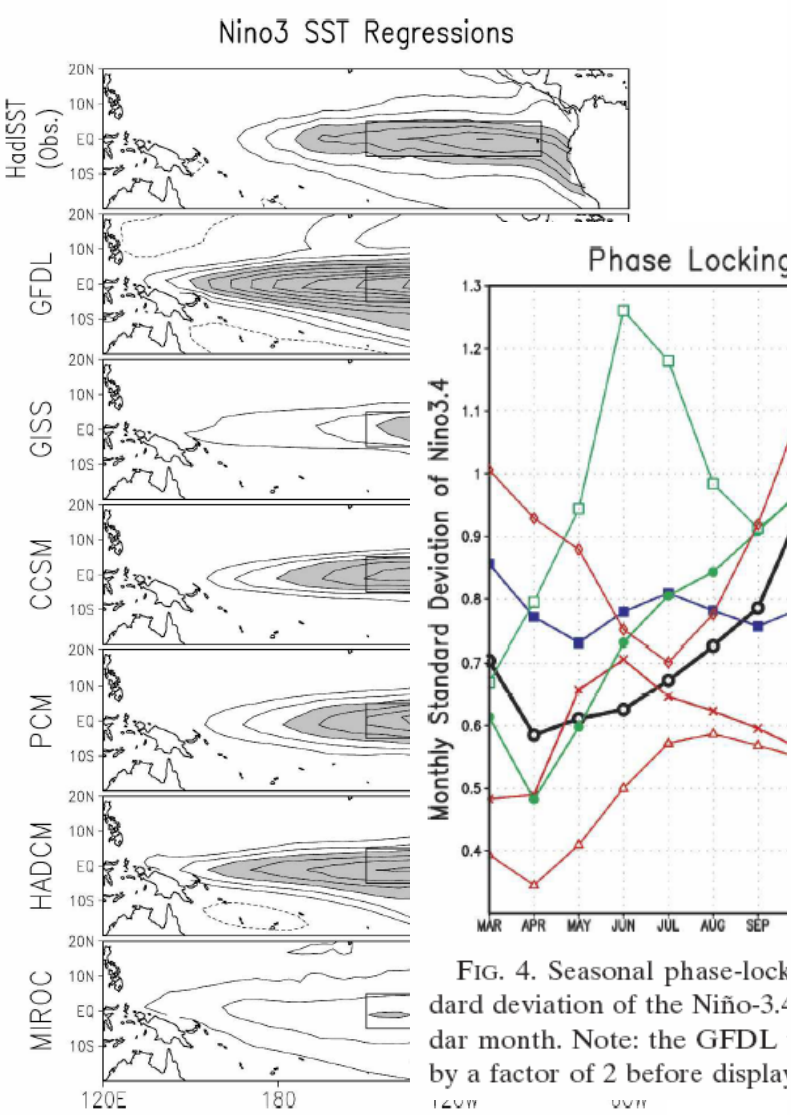

FIG. 4. Seasonal phase-lock
dard deviation of the Niño-3.4
dar month. Note: the GFDL
by a factor of 2 before displa

FIG. 1. Niño-3 SST index regressions on observed and simulated SSTs in the 1950–99 period, based on all calendar month anomalies. The marked rectangular box outlines the Niño-3 region (5°S–5°N, 150°–90°W). SST observations are from the HadISST analysis. Simulating models are noted at the left of each panel. The contour interval is 0.2 K and the zero contour is suppressed; the shading threshold is 0.6 K.

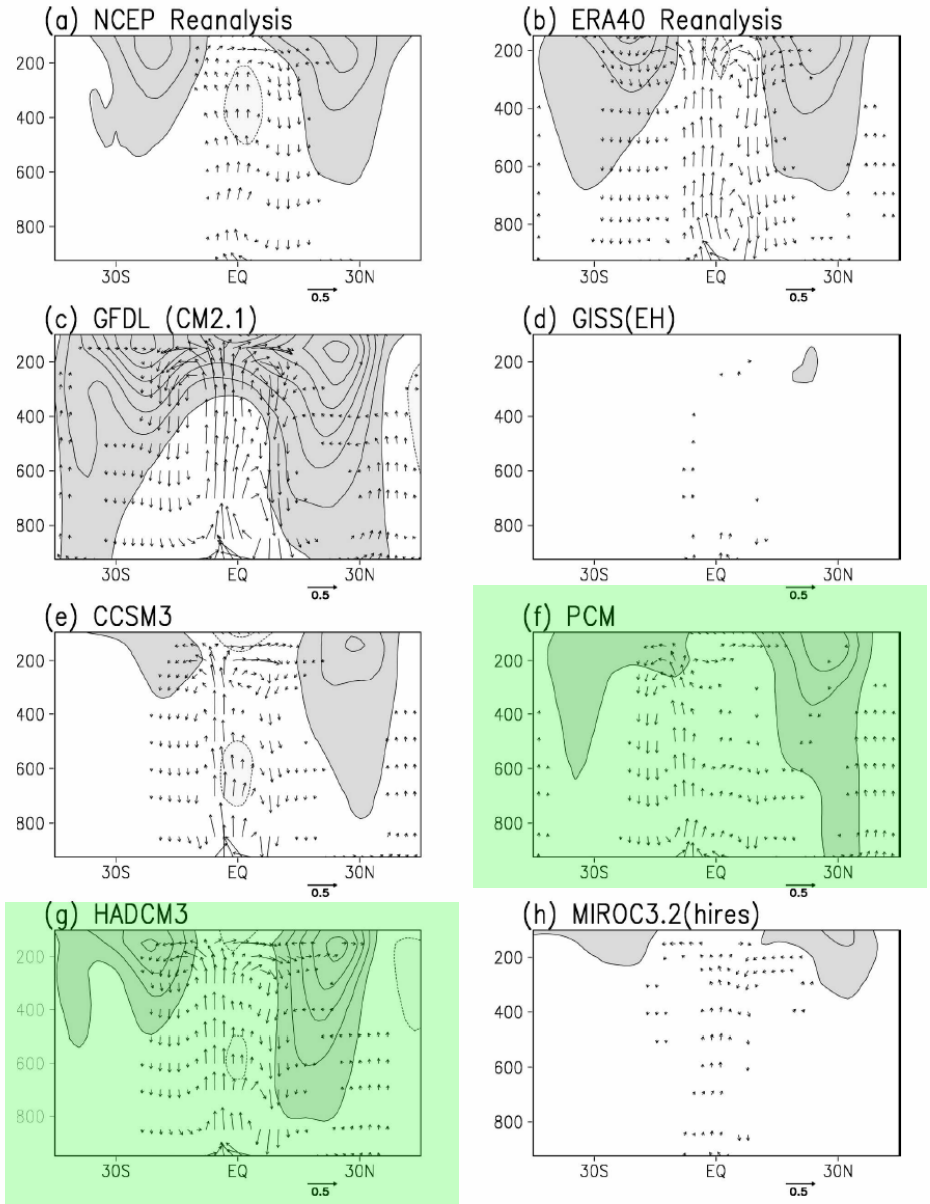

FIG. 8. ENSO's zonally symmetric winter circulation response in the Tropics/subtropics: Niño-3 SST index regressions on zonal-mean zonal wind (rotational flow) are shown using a contour interval and a shading threshold of 0.5 m s^{-1}; the zero contour is omitted in all panels. Regressions on divergent (Hadley) circulation are shown using vectors, whose zonal component denotes zonal-mean meridional wind (in m s^{-1}) and whose vertical component denotes the zonal-mean vertical velocity (in Pa h^{-1}). Vectors of magnitude less than 0.05 are suppressed. The same vector scale, shown below the panels, is used in all cases. Light (dark) shading denotes negative (positive) values.

Basic SST-SLP coupled relationship (Bjerknes' mechanism)…

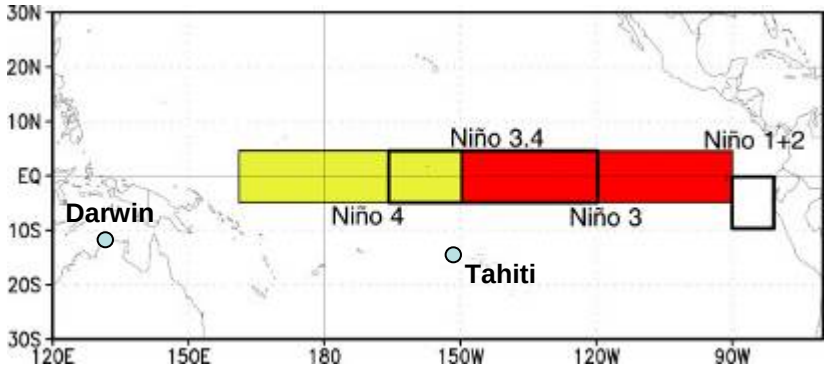

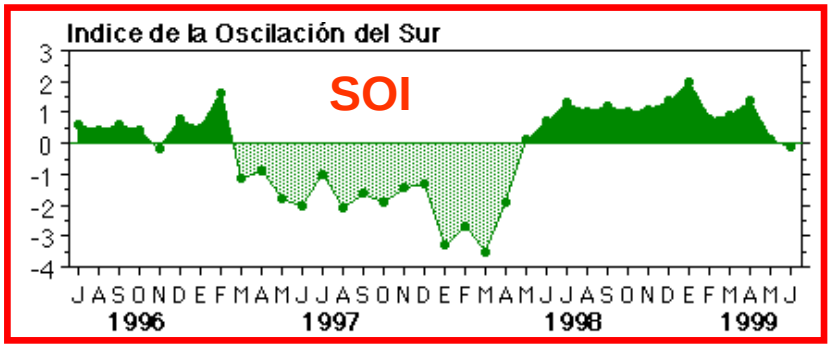

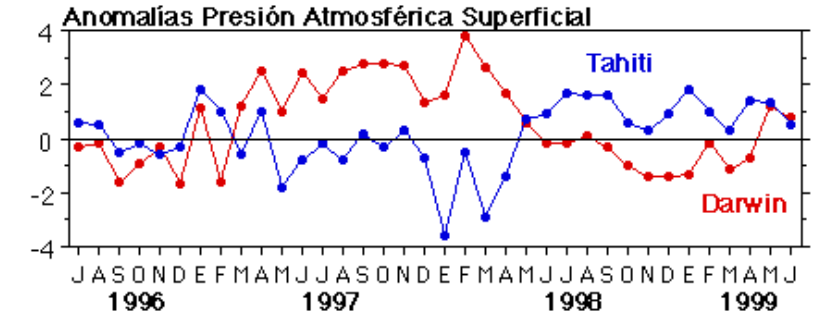

Preparado por el Dpto. de Geofísica,
U. de Chile, con datos del NCEP/NOAA

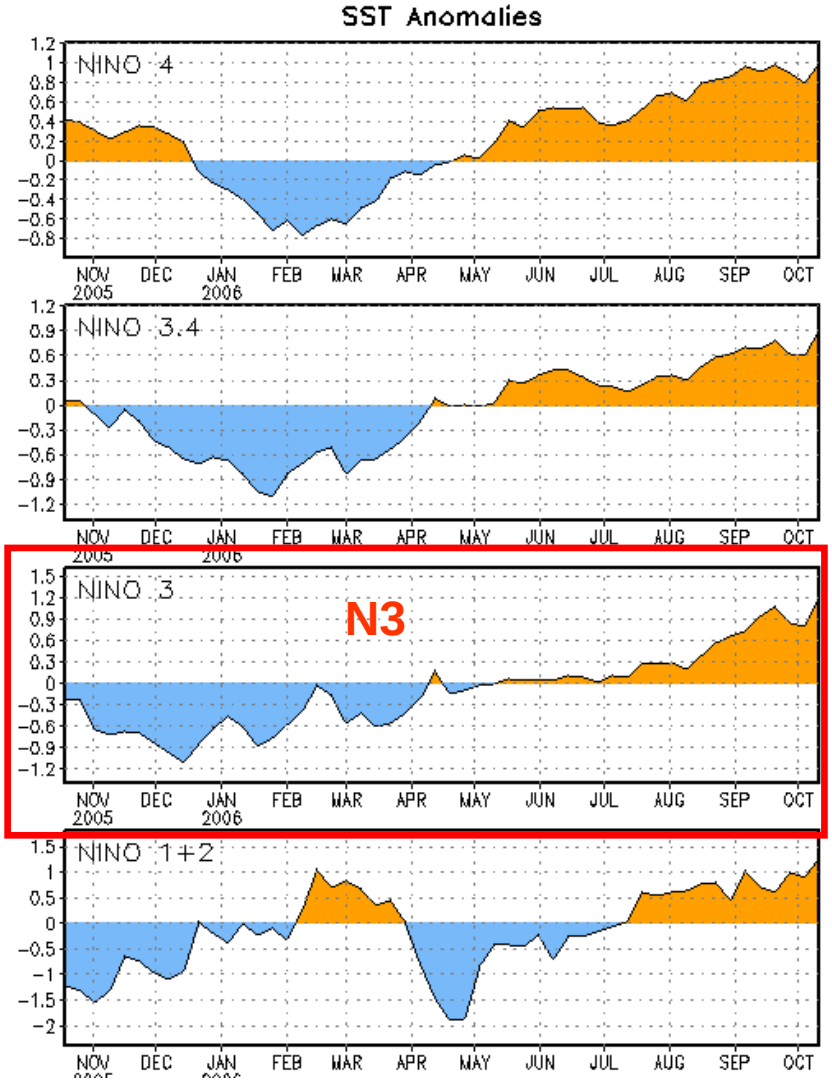

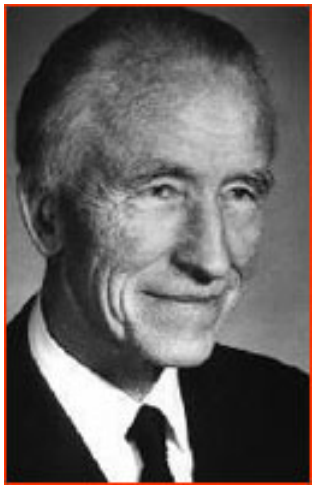

Jacob Bjerknes

... A change toward a steeper pressure slope at the base of the Walker Circulation is associated with an increase in the equatorial easterly winds and hence also with an increase in the upwelling and a sharpening of the contrast of surface temperature between the eastern and western equatorial Pacific. This chain reaction shows that an intensifying Walker Circulation also provides for an increase of the east-west temperature contrast that is the cause of the Walker Circulation in the first place. On the other hand, a case can also be made for a trend of decreasing speed of the Walker Circulation ...

Bjerknes 1969

Observed (**raw** data)

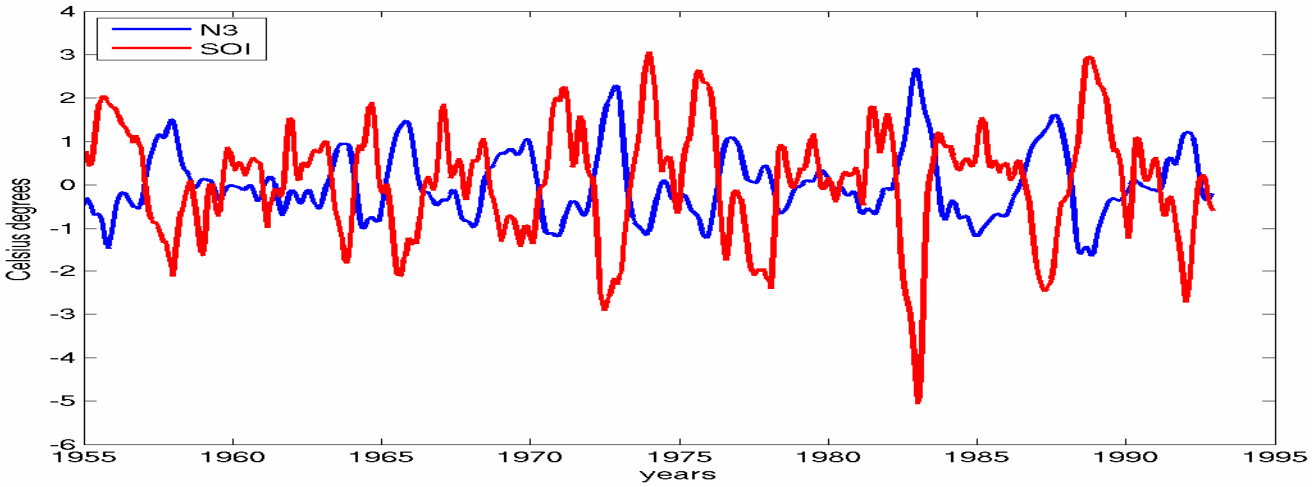

r = -0,83

σ_{SOI} = 1,31 hPa

σ_{N3} = 0,79 °C

Observed (**raw** data)

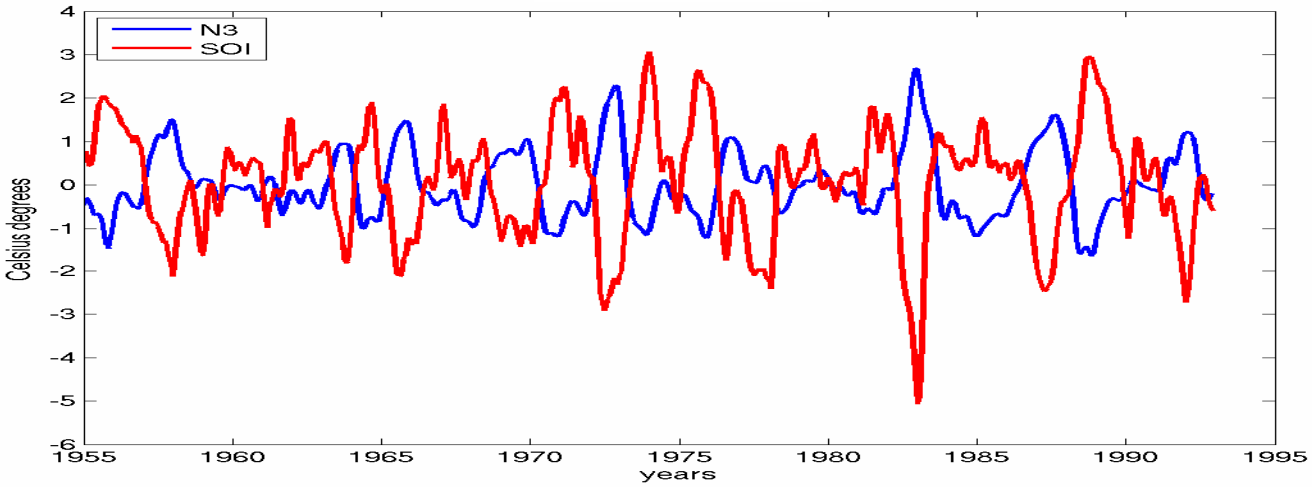

r = -0,83

σ_{SOI} = 1,31 hPa

σ_{N3} = 0,79 °C

Combined Complex Empirical Orthogonal Function

Observed (**raw** data)

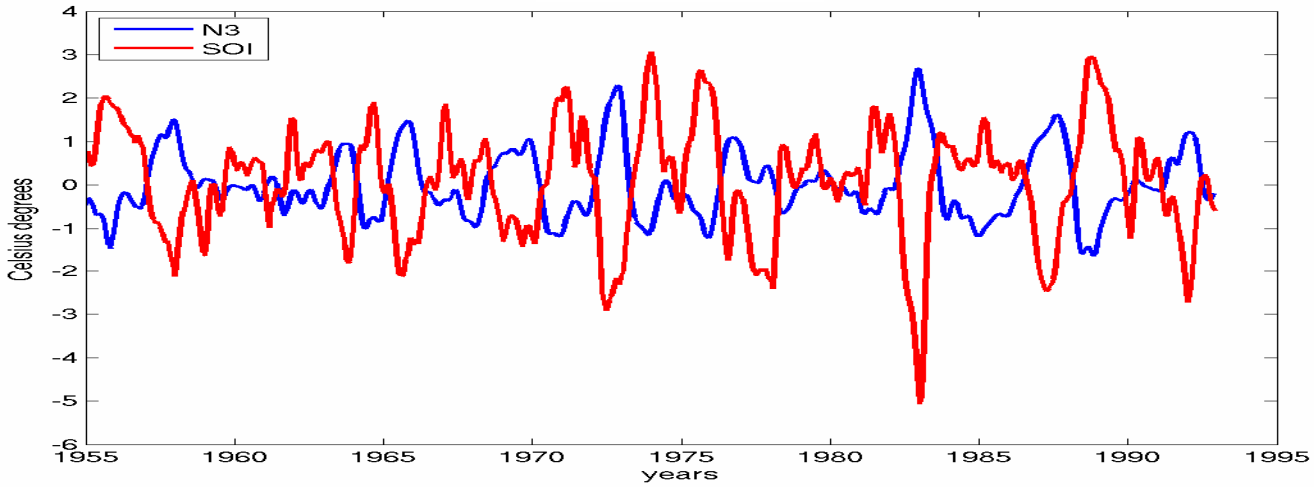

r = -0,83

σ_{SOI} = 1,31 hPa

σ_{N3} = 0,79 °C

Combined Complex Empirical Orthogonal Function

Reconstructed from the first **CCEOF1 mode**

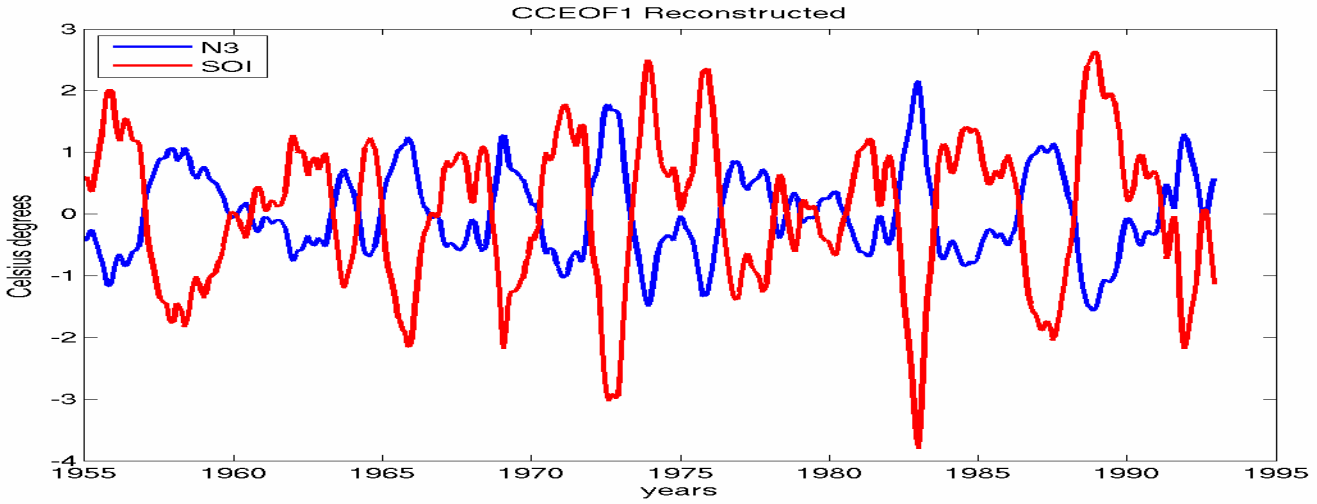

$\%_{mode1}$ = 42%

r = -1,0

σ_{SOI} = 1,21 hPa

σ_{N3} = 0,71 °C

IPCC-AR4 models used in this study.

Model Name	Short Name	Originating group(s)	Atmosphere Resolution (lat x lon)		Ocean Resolution (lat x lon)		Atm. Vertical Levels	Oce. Vertical Levels	Flux correction
BCCR-BCM2.0	BCCR	Bjerknes Centre/Norway	~2.8°	~2.8°	0.5°-1.5°	1.5°	31	35	None
CGCM3.1(T63)	CGCM3	CCCMA/Canada	~3.75°	3.75°	~1.85°	1.85°	31	29	*2
CCSM3.1	CCSM3	NCAR/USA	~1.4°	~1.4°	~0.27°	1.125°	26	40	None
CSIRO-Mk3.0	CSIRO	CSIRO/Australia	~1.88°	~1.88°	~0.84°	~1.88°	18	31	None
ECHAM5/MPI-OM	ECHAM5	MPI/Germany	~1.88°	~1.88°	~1.5°	~1.5°	31	40	None
FGOALS-g1.0	FGOALS	IAP/China	~2.8°	~2.8°	1°	1°	26	33	None
GFDL-CM2.0	GFDL	GFDL/USA	2°	2.5°	1/3°-1°	1°	24	50	None
GISS-AOM	GISSAOM	NASA-GISS/USA	3°	4°	3°	4°	12	16	None
GISS-EH	GISSEH	NASA-GISS/USA	4°	5°	2°	2°	20	16	None
UKMO-HadCM3	HADCM3	Met Office/UK	2.5°	3.75°	1.25°	1.25°	19	20	None
UKMO-HadGEM1	HADGEM	Met Office/UK	1.25°	~1.88°	1/3°-1°	1°	38	40	None
MIROC3.2(hires)	HIRES	CCSR-NIES-FRCGC/Japan	~1.125°	1.125°	~0.18°	~0.28°	56	47	None
INM-CM3.0	INMCM	INM/Russia	4°	5°	2°	2.5°	21	33	*1
IPSL-CM4	IPSL	IPSL/France	2.5°	3.75°	1°	2°	19	31	None
MIROC3.2(medres)	MEDRES	CCSR-NIES-FRCGC/Japan	~2.8°	~2.8°	0.5°-1.4°	1.4°	20	43	None
MRI-CGCM2.3.2	MRI	MRI/Japan	~2.8°	~2.8°	0.5°-2°	2.5°	30	23	*3
PCM	PCM	NCAR/USA	~2.8°	~2.8°	0.5°	0.7	26	40	None

*1 Water (Greenland/Iceland/Norwegian, Barentz and Kara Seas);
*2 Heat and water; *3 Heat and water (global), momentum (12°N-12°S)

Reconstructed Niño 3 SST from the first SST-SLP combined complex empirical orthogonal function (CCEOF1) mode in the South Pacific Ocean – ENSO TIMESCALE

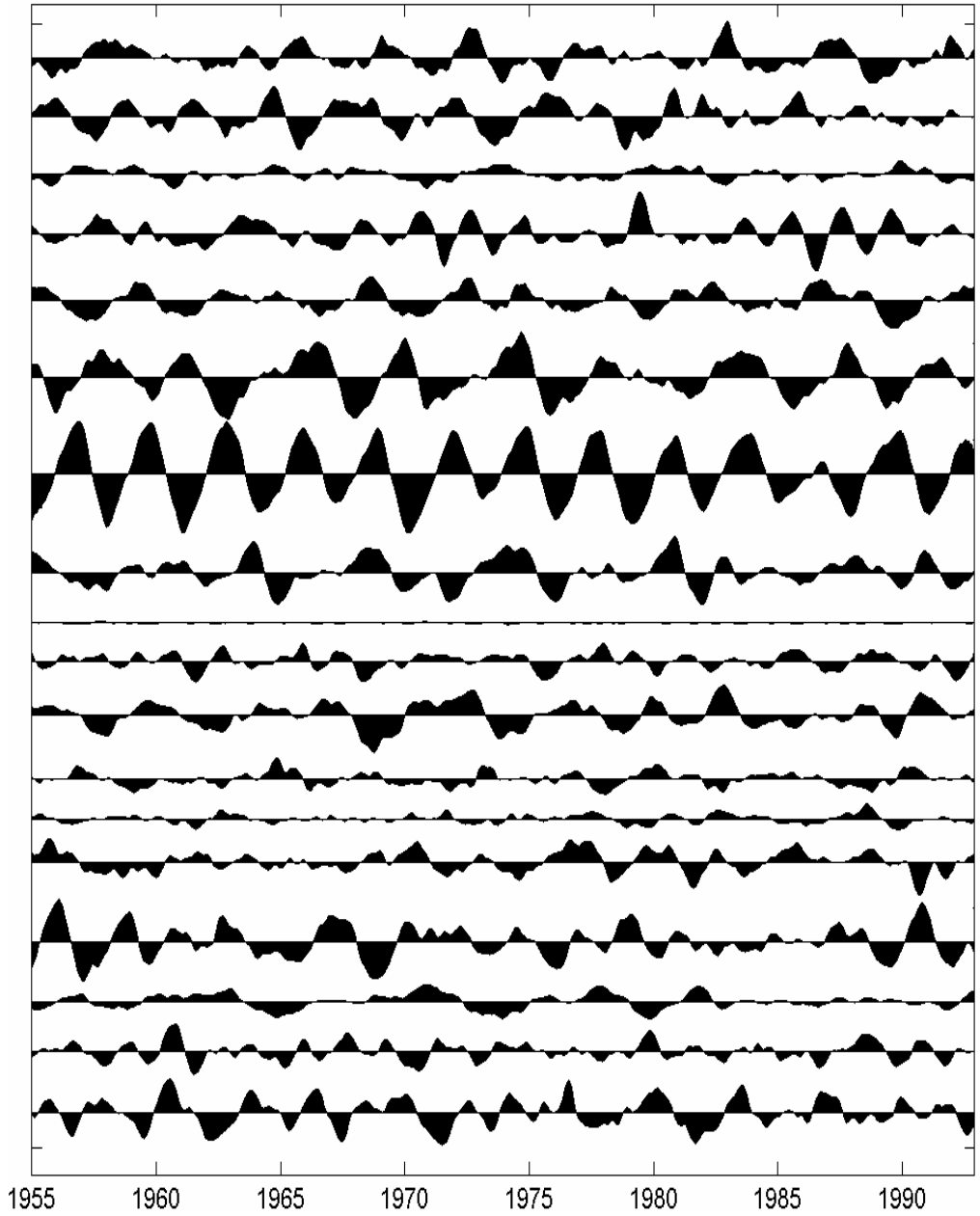

	σ_{N3}	σ_{SOI}	$r_{N3.SOI}$	$\%_{modo1}$
OBS	0,71	1,21	~ -1	42
BCCR	0,78	0,39	-0,93	21
CGCM3	0,32	0,73	~ -1	25
CCSM3	0,74	0,35	~ -1	25
CSIRO	0,65	0,80	-0,80	32
ECHAM5	1,14	0,83	~ -1	40
FGOALS	1,78	0,84	-0,95	49
GFDL	0,82	0,87	-0,99	41
GISSAOM	0,03	0,12	-0,76	26
GISSEH	0,46	0,14	-0,15	19
HADCM3	0,78	0,87	~ -1	32
HADGEM	0,38	0,53	-0,92	24
HIRES	0,25	0,58	-0,96	25
INMCM	0,61	0,17	-0,88	25
IPSL	0,94	0,26	-0,91	30
MEDRES	0,43	0,46	-0,99	35
MRI	0,51	0,76	~ -1	37
PCM	0,81	0,40	-0,98	23

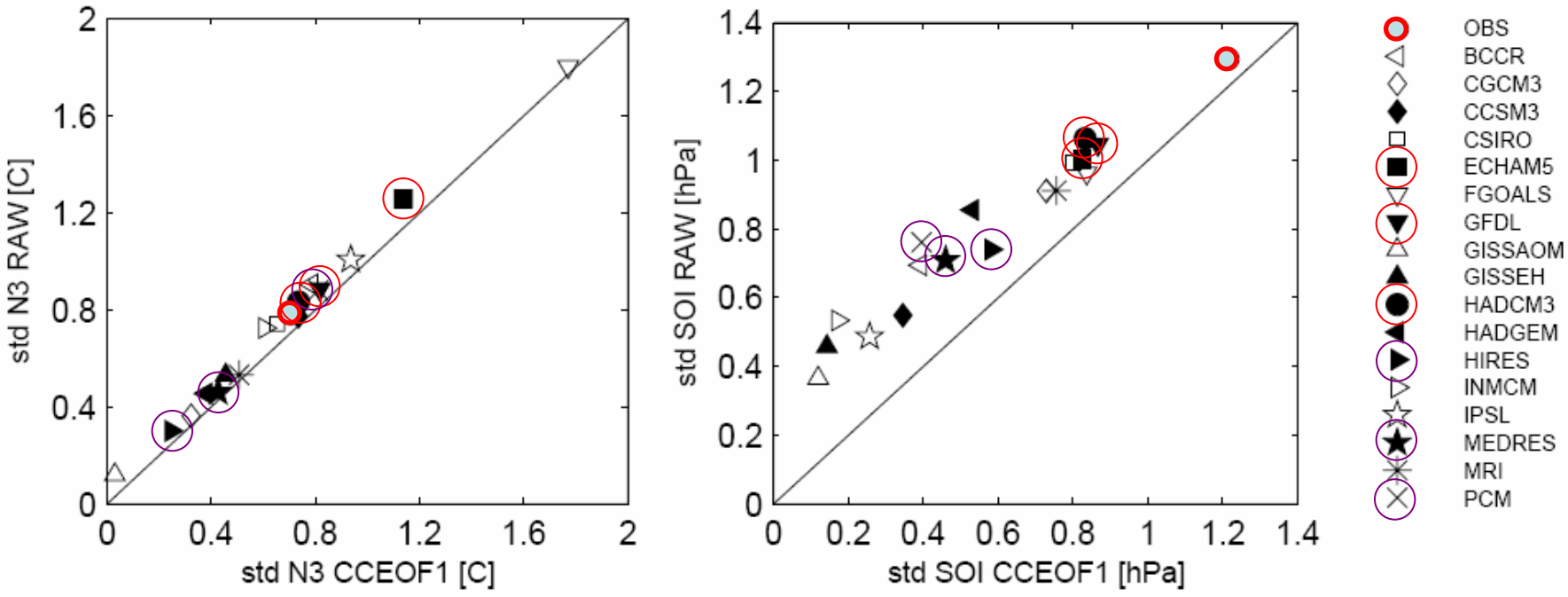
std N3 RAW [C]
std N3 CCEOF1 [C]
0
0.4
0.8
1.2
1.6
2
std SOI RAW [hPa]
std SOI CCEOF1 [hPa]
0.2
0.6
1
1.4
OBS
BCCR
CGCM3
CCSM3
CSIRO
ECHAM5
FGOALS
GFDL
GISSAOM
GISSEH
HADCM3
HADGEM
HIRES
INMCM
IPSL
MEDRES
MRI
PCM

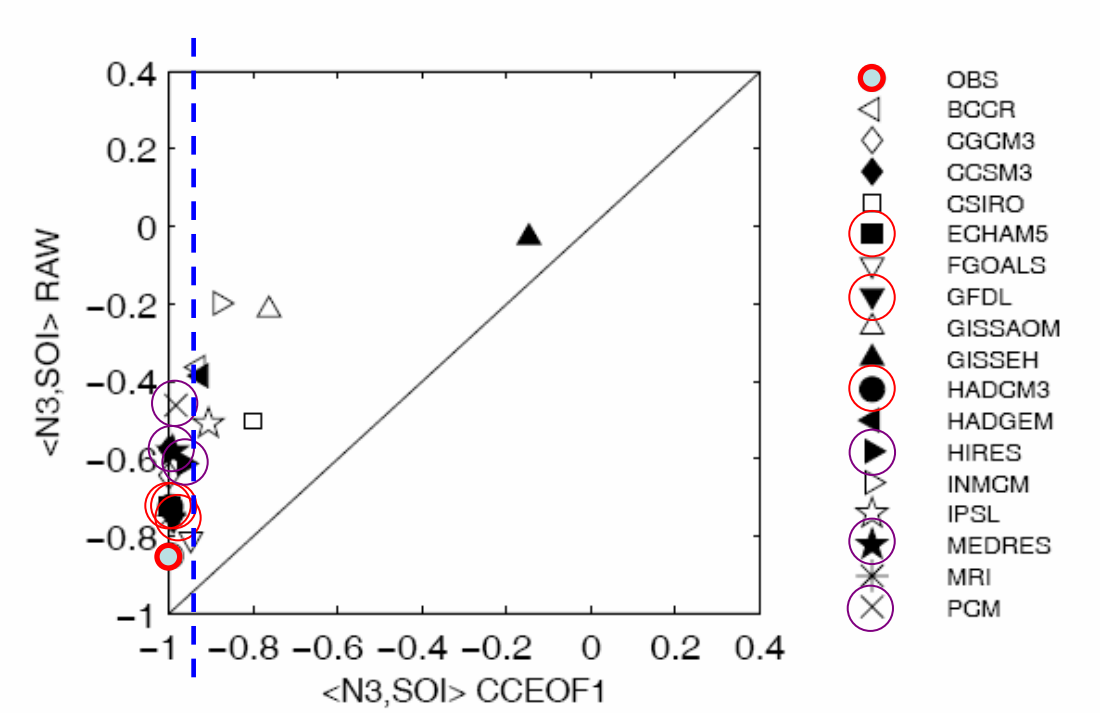
0.4
0.2
0
−0.2
−0.4
−0.6
−0.8
−1
−1
−0.8
−0.6
−0.4
−0.2
0
0.2
0.4
<N3,SOI> RAW
<N3,SOI> CCEOF1
OBS
BCCR
CGCM3
CCSM3
CSIRO
ECHAM5
FGOALS
GFDL
GISSAOM
GISSEH
HADCM3
HADGEM
HIRES
INMCM
IPSL
MEDRES
MRI
PCM

ENSO pattern, teleconnections, impacts

HIRES

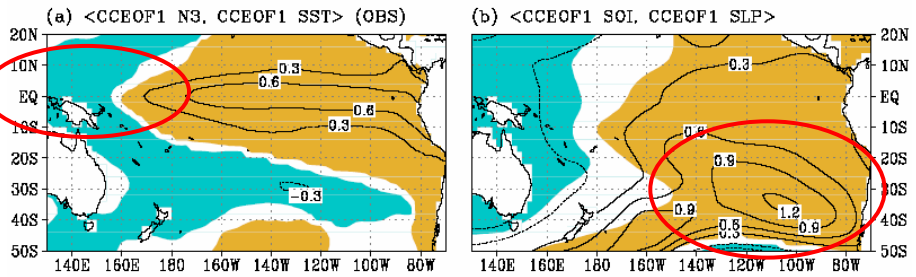

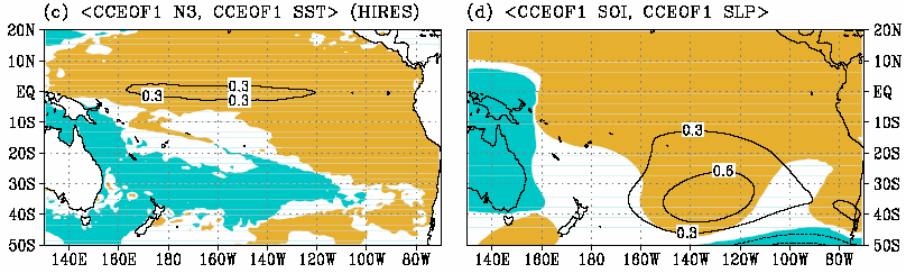

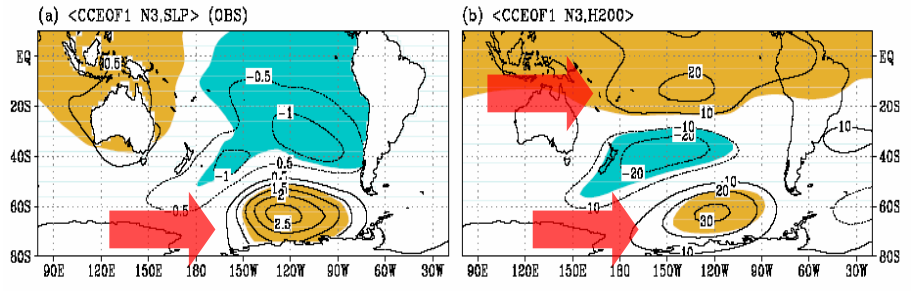

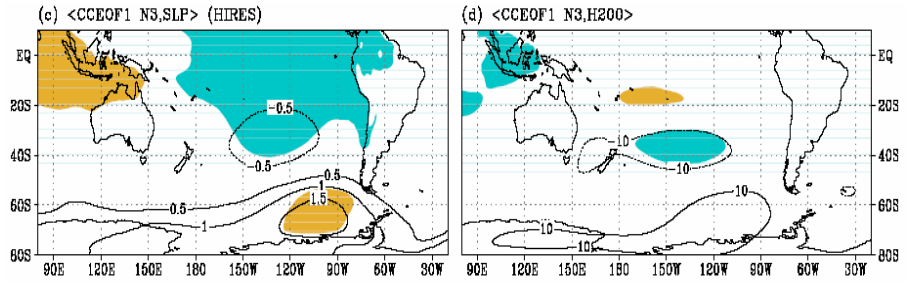

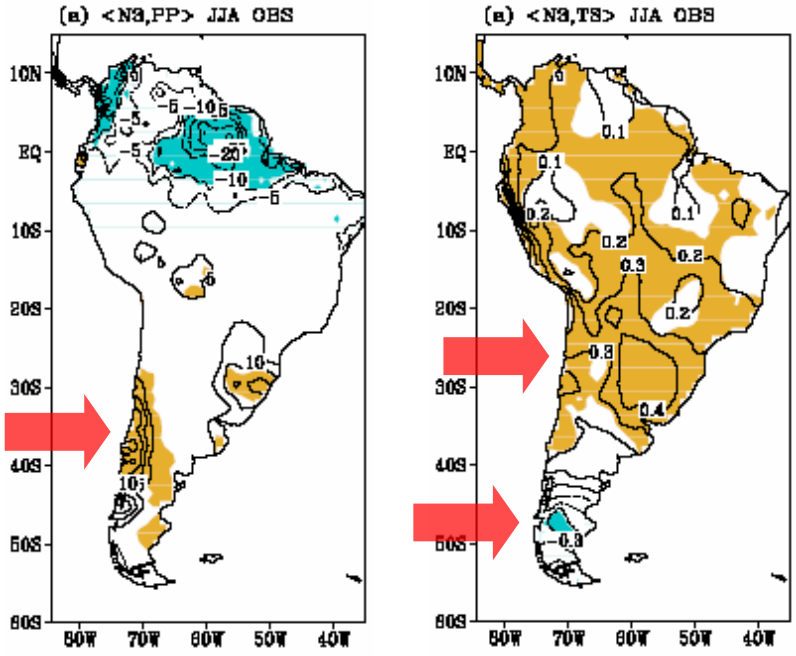

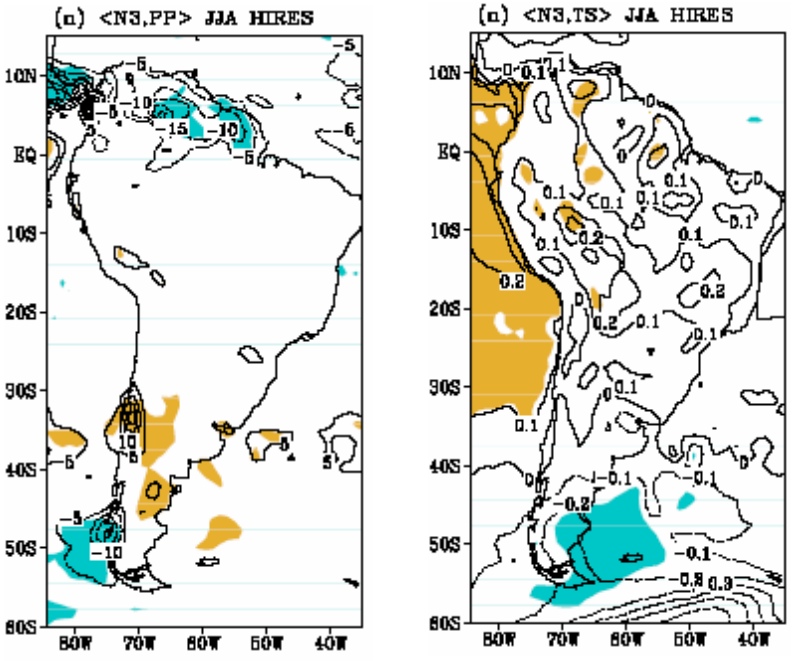

ENSO pattern, teleconnections, impacts

MEDRES

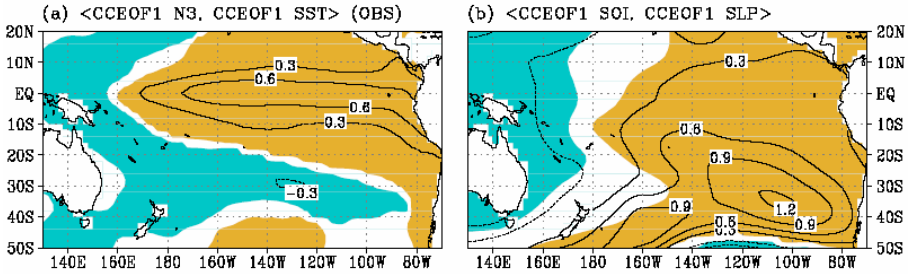

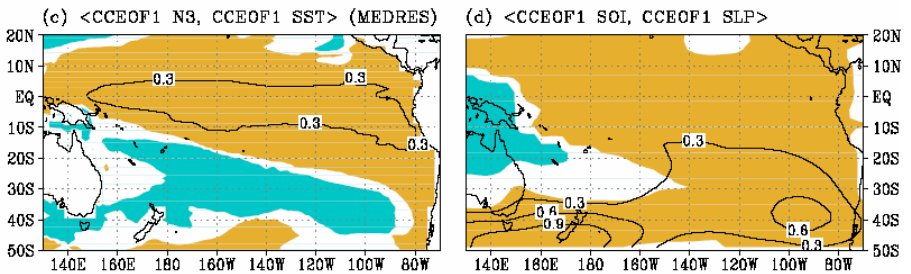

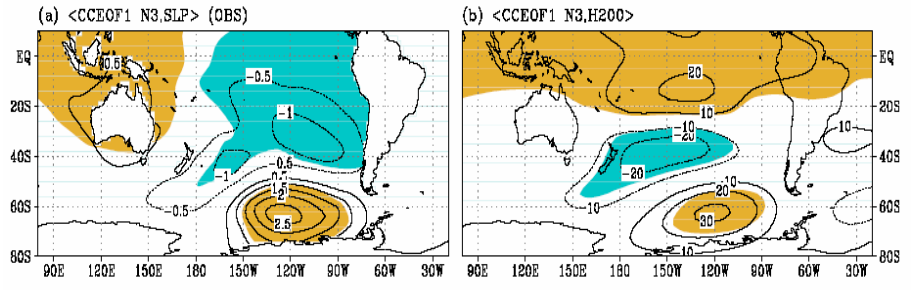

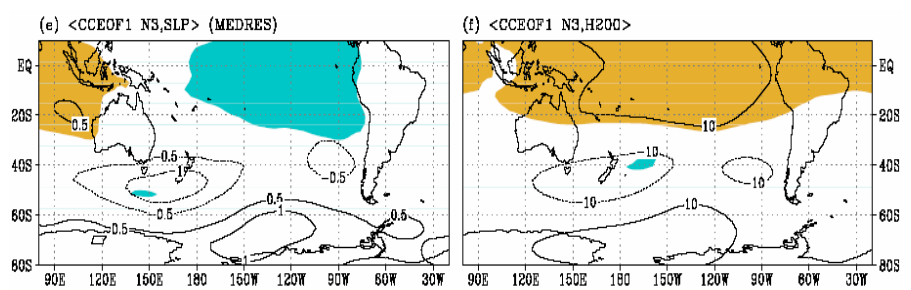

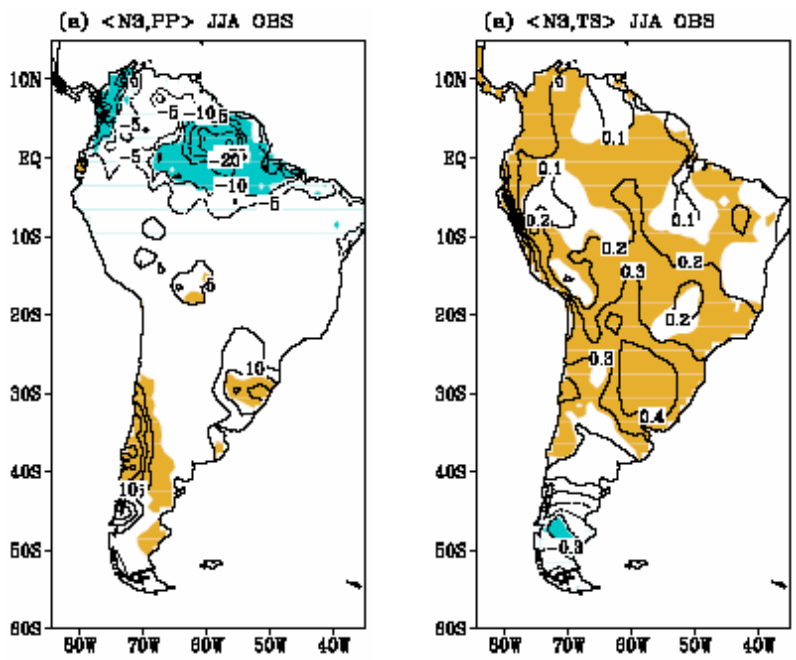

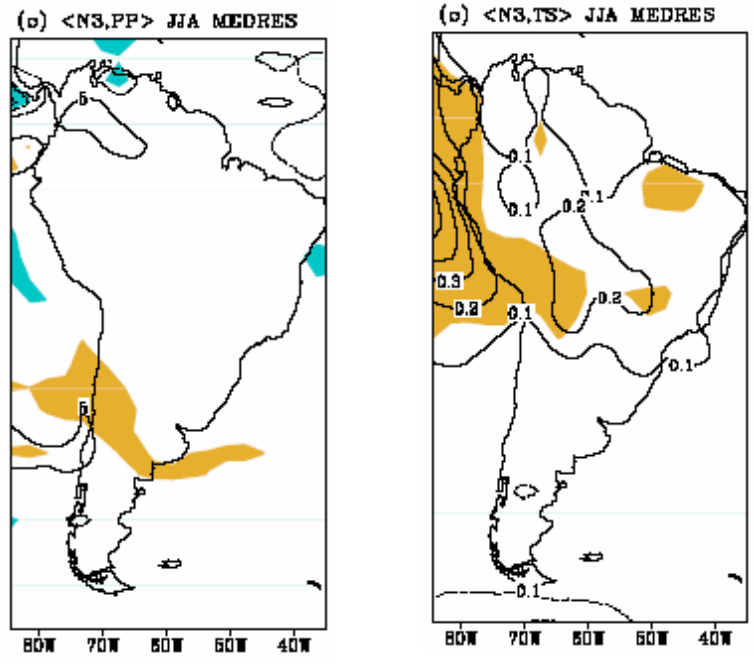

ENSO pattern, teleconnections, impacts

PCM

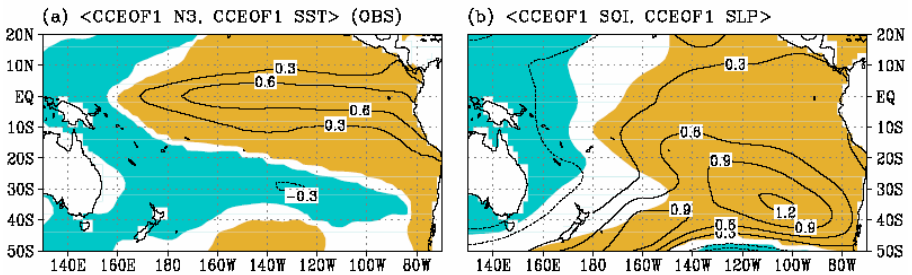

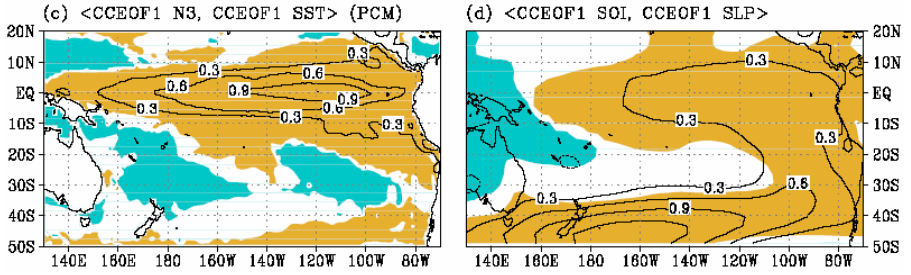

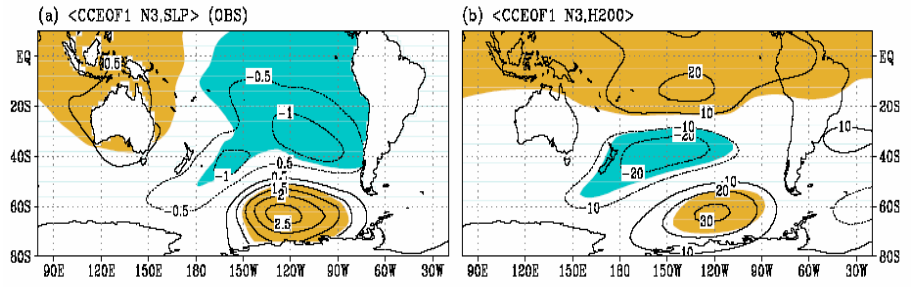

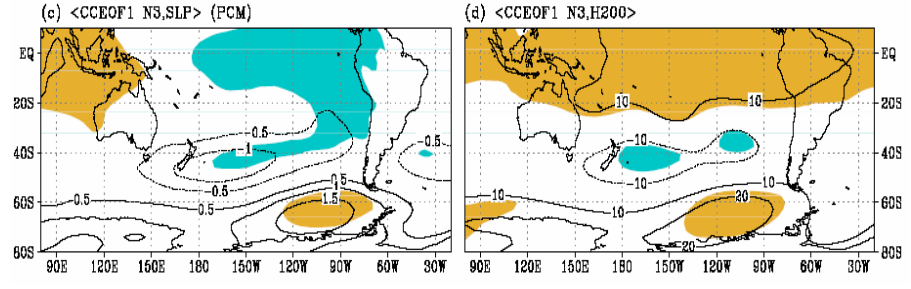

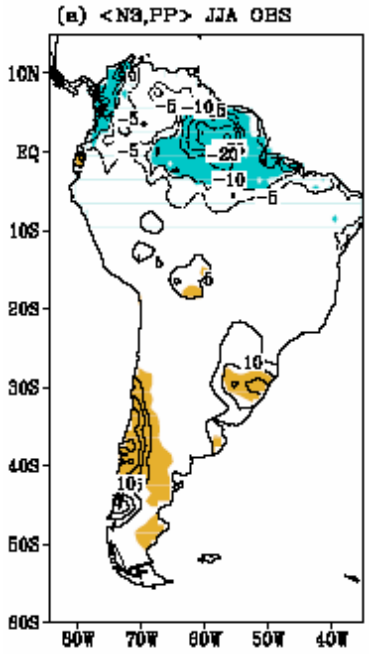

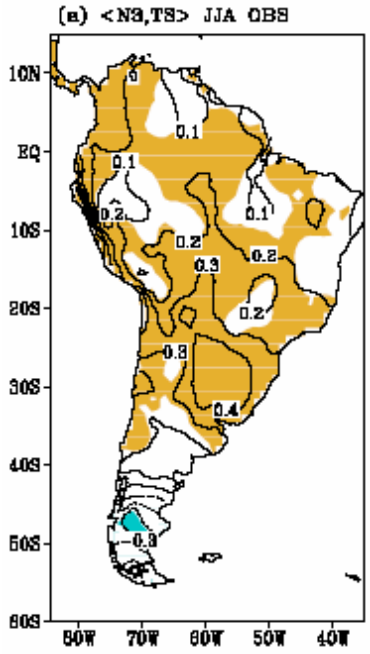

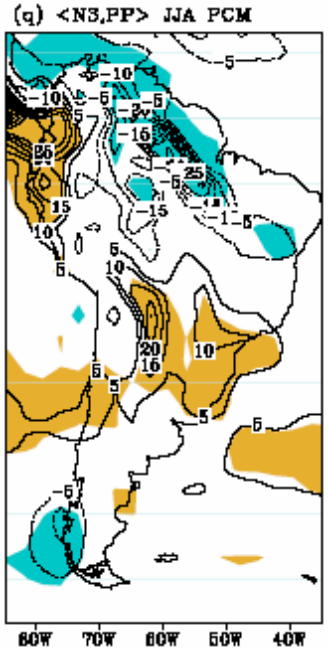

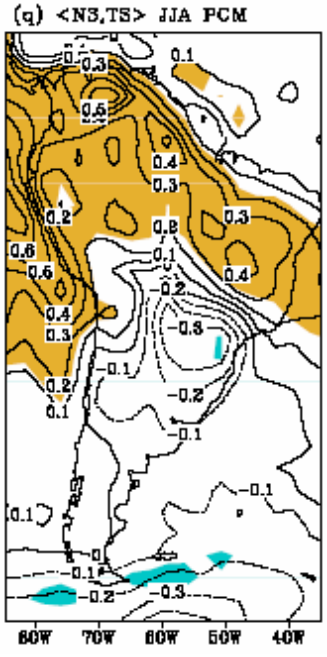

ENSO pattern, teleconnections, impacts

ECHAM5

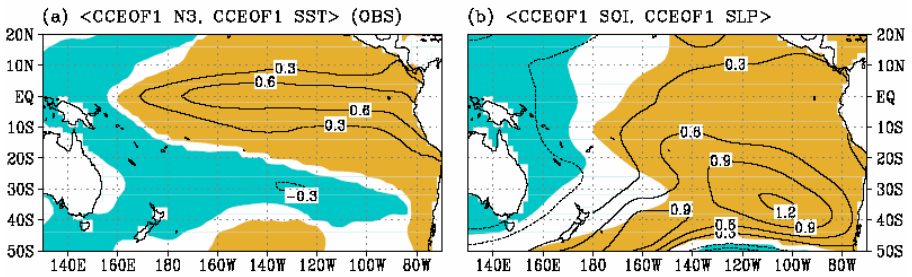

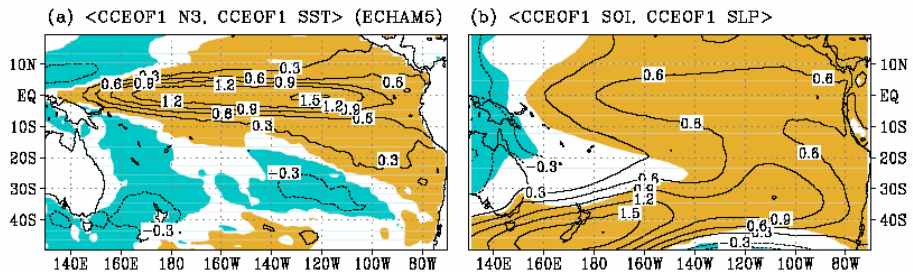

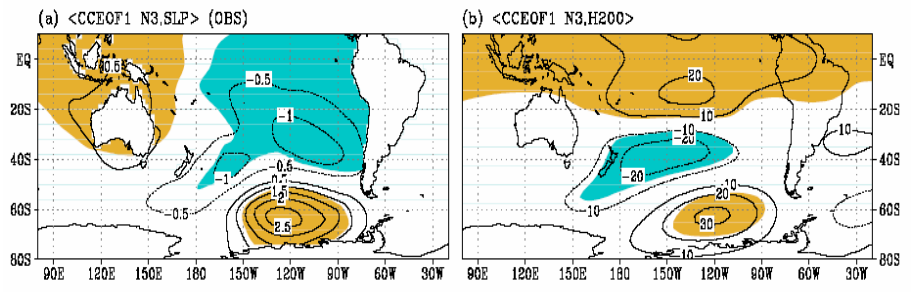

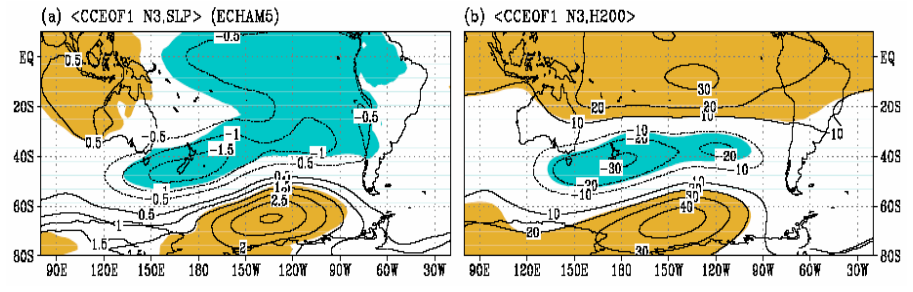

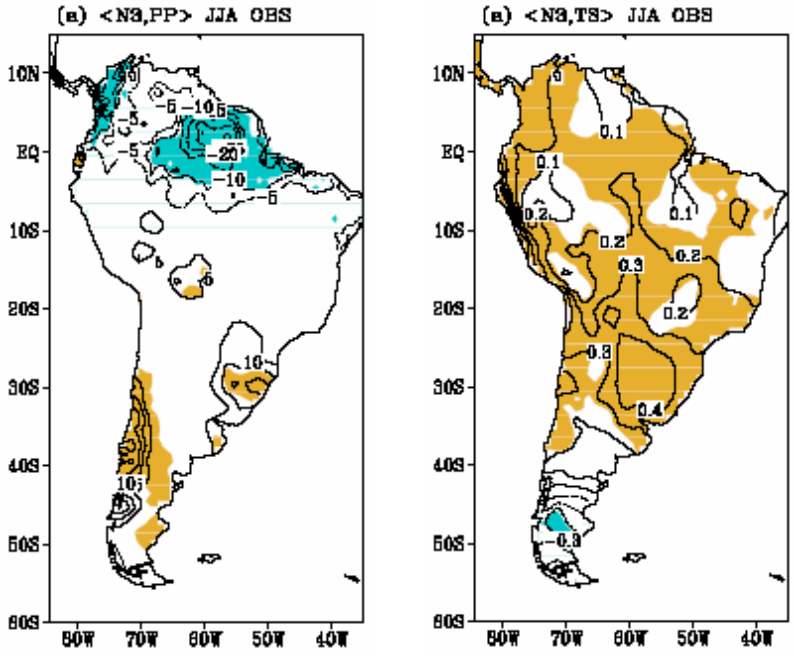

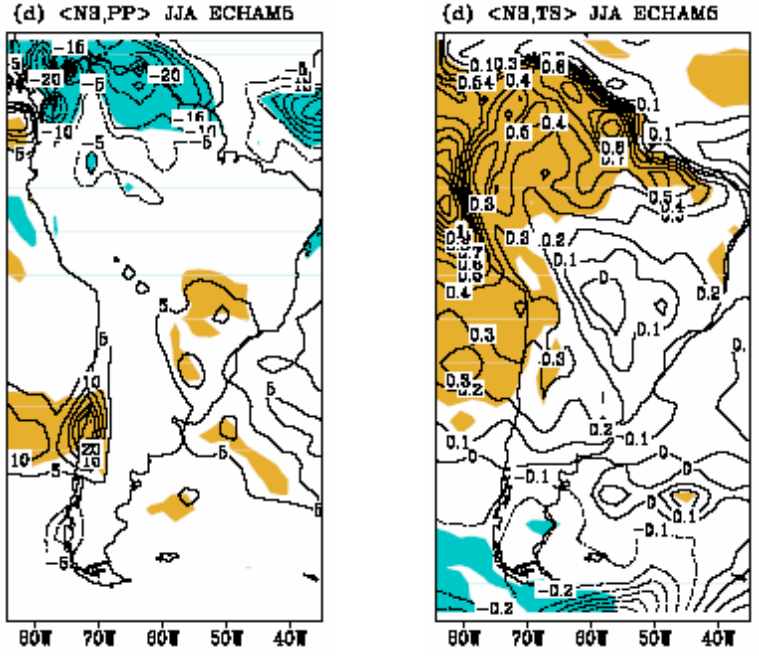

ENSO pattern, teleconnections, impacts

HADCM3

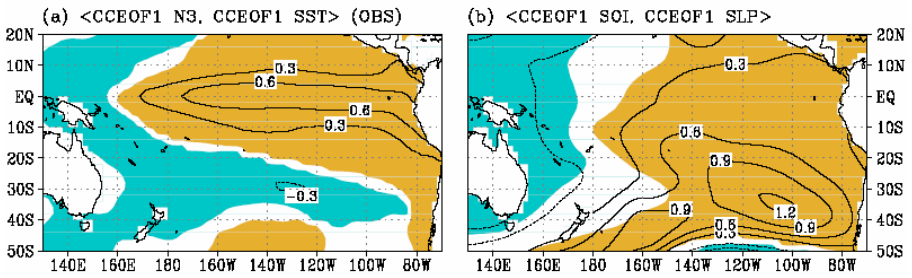

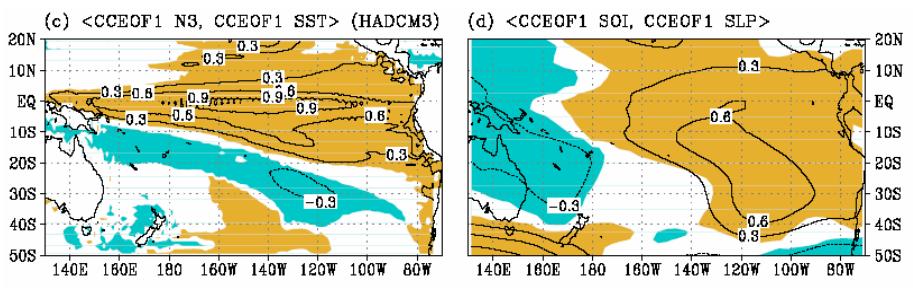

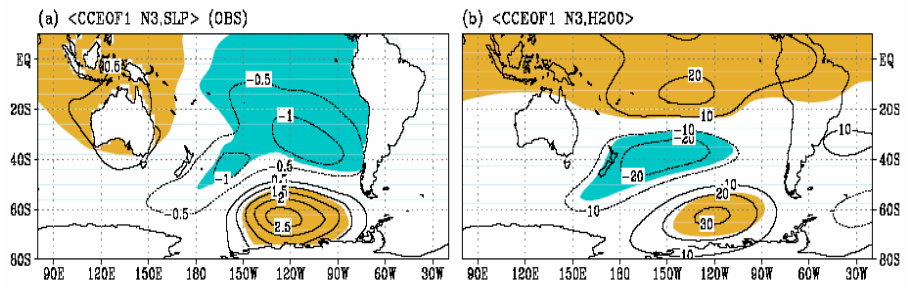

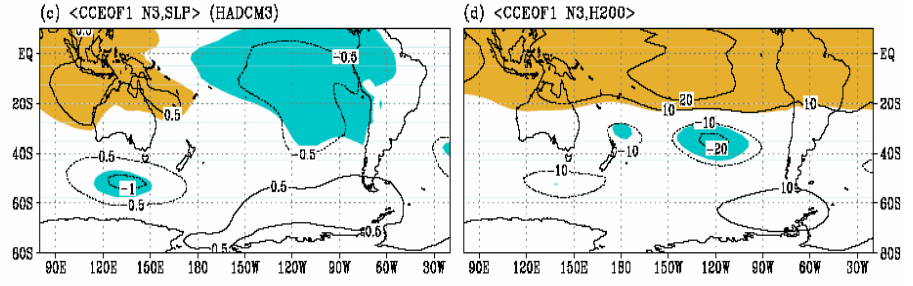

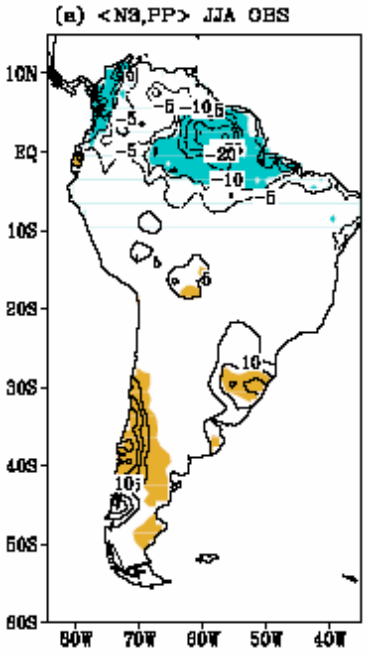

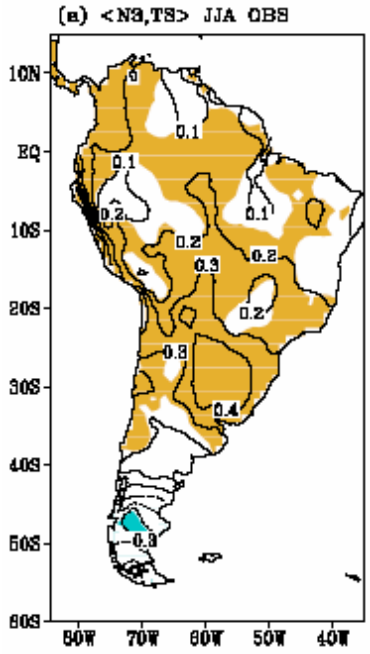

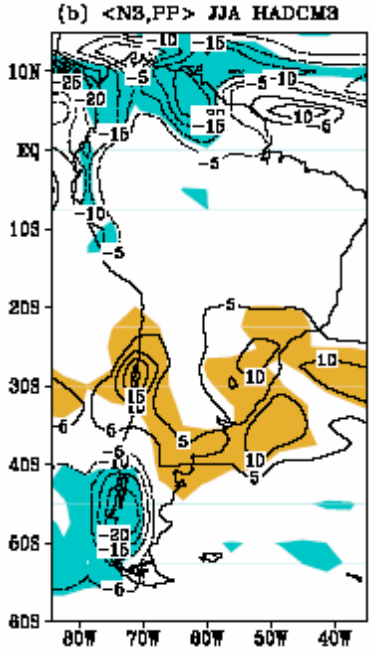

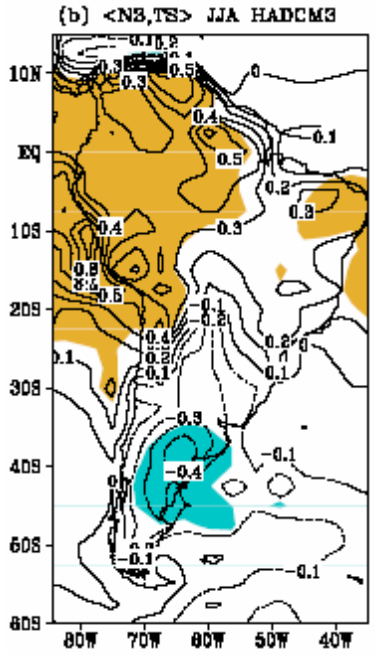

ENSO pattern, teleconnections, impacts

HADCM3

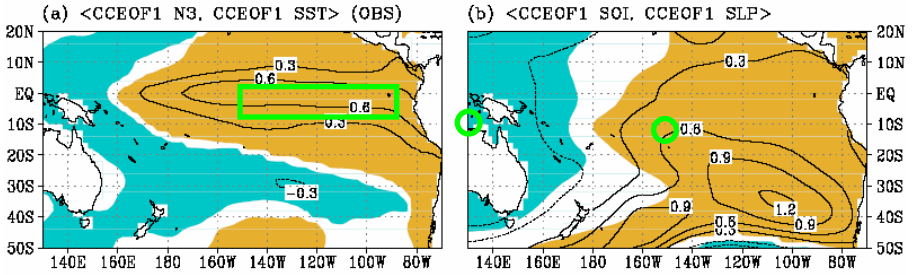

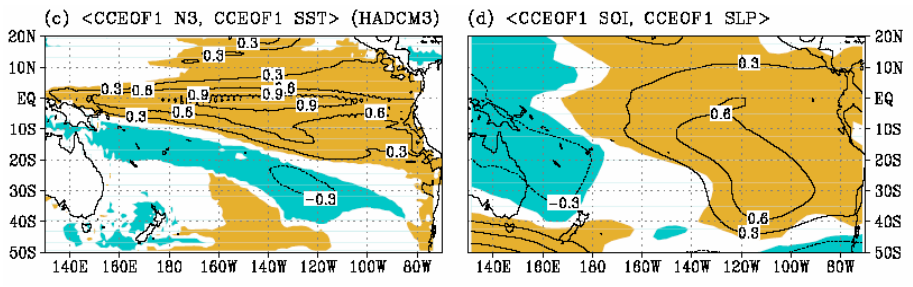

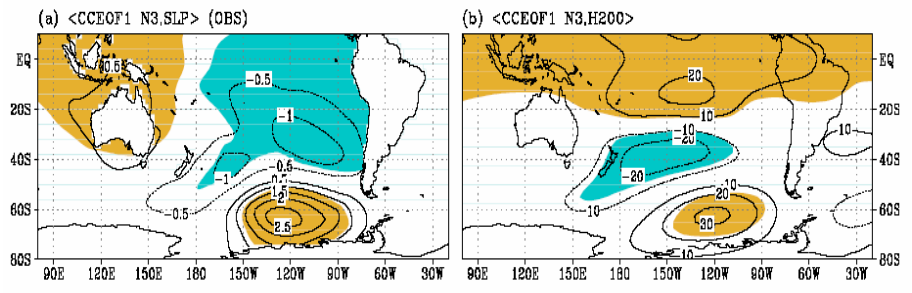

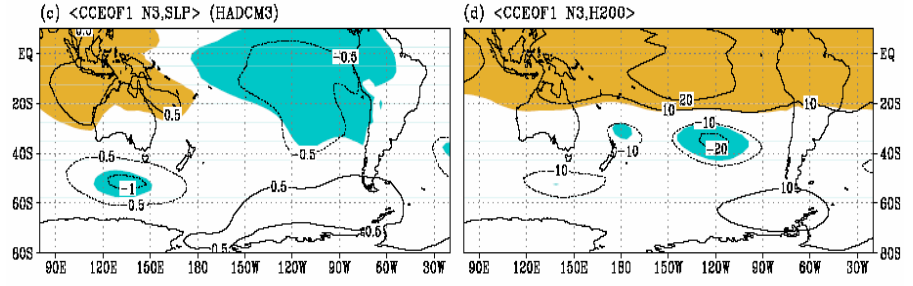

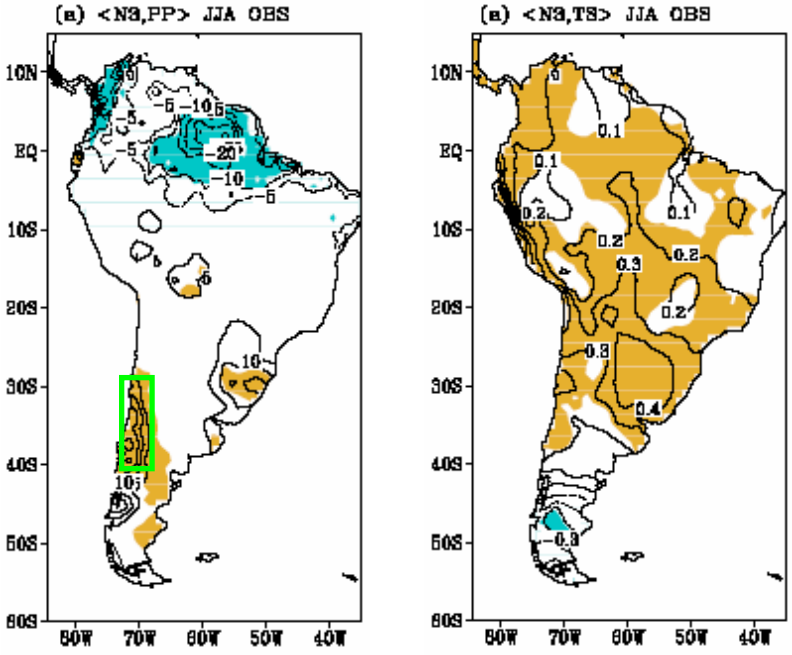

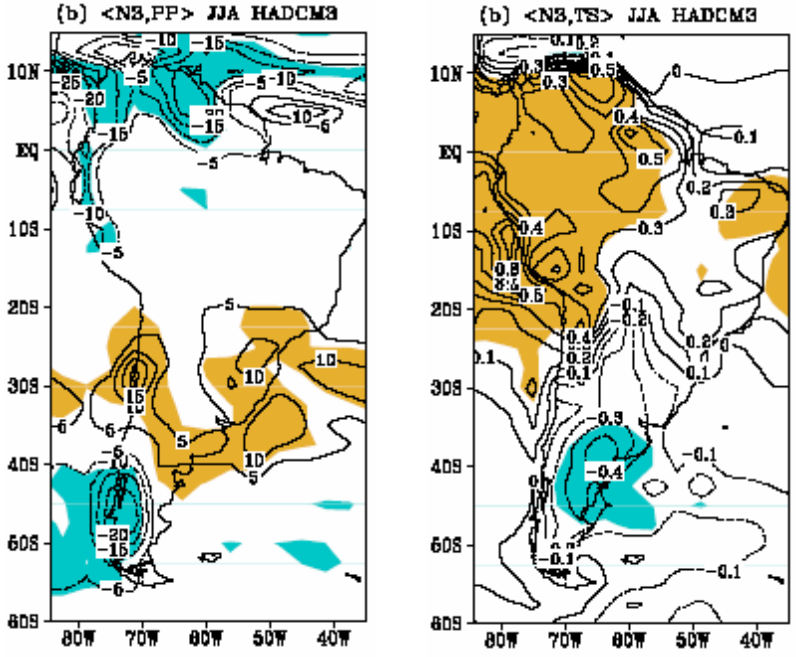

ENSO pattern, teleconnections, impacts

HADCM3

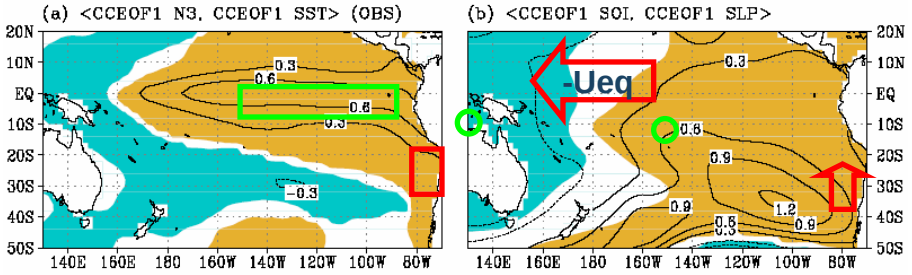

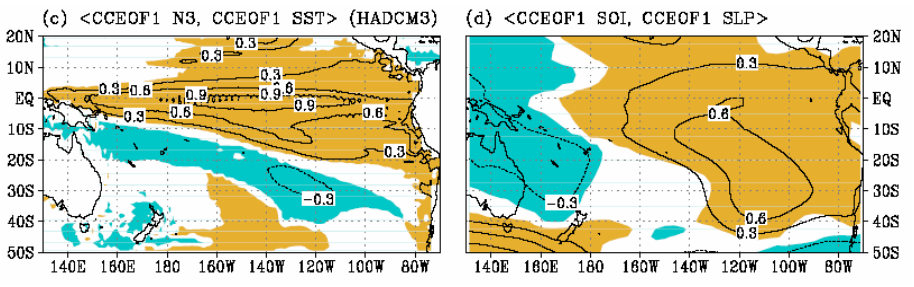

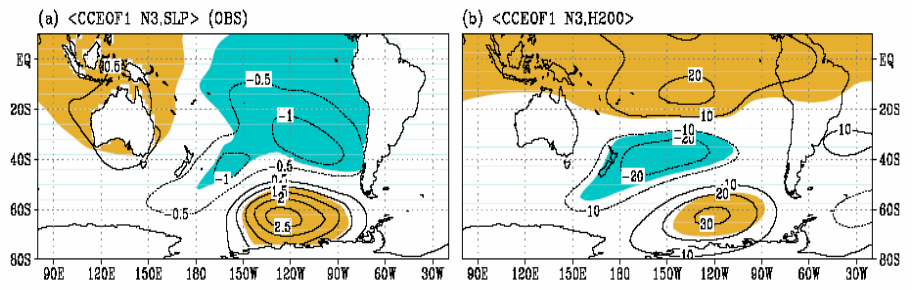

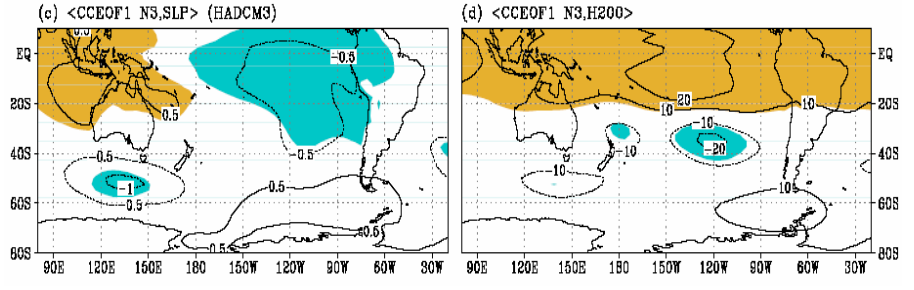

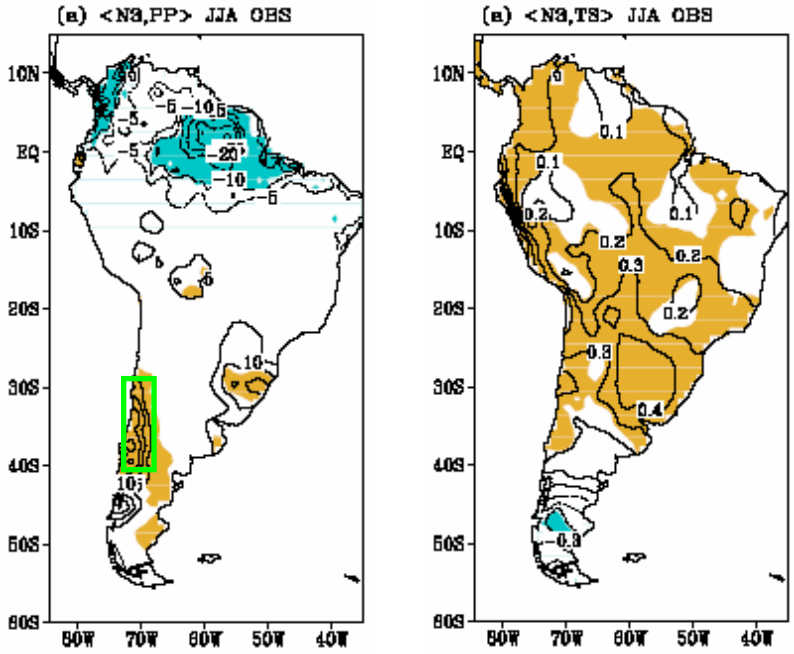

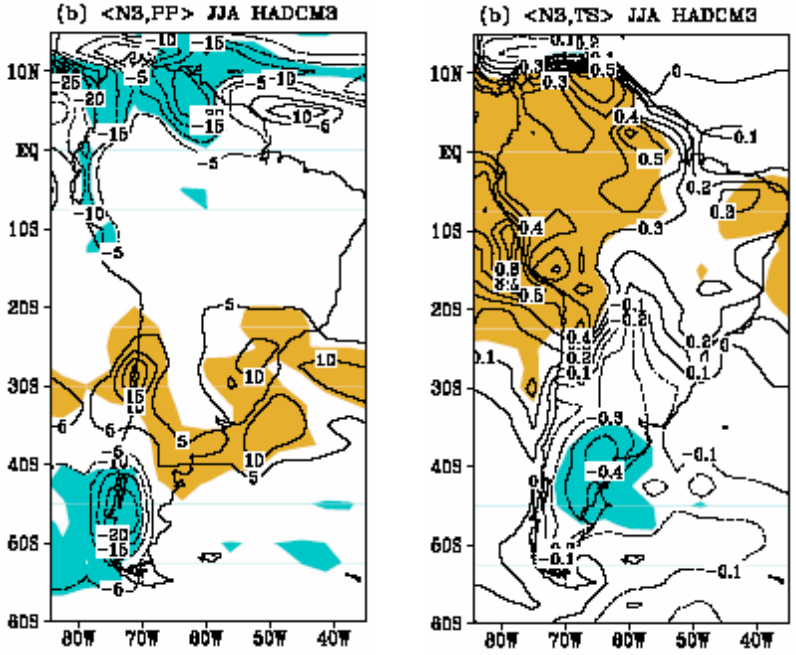

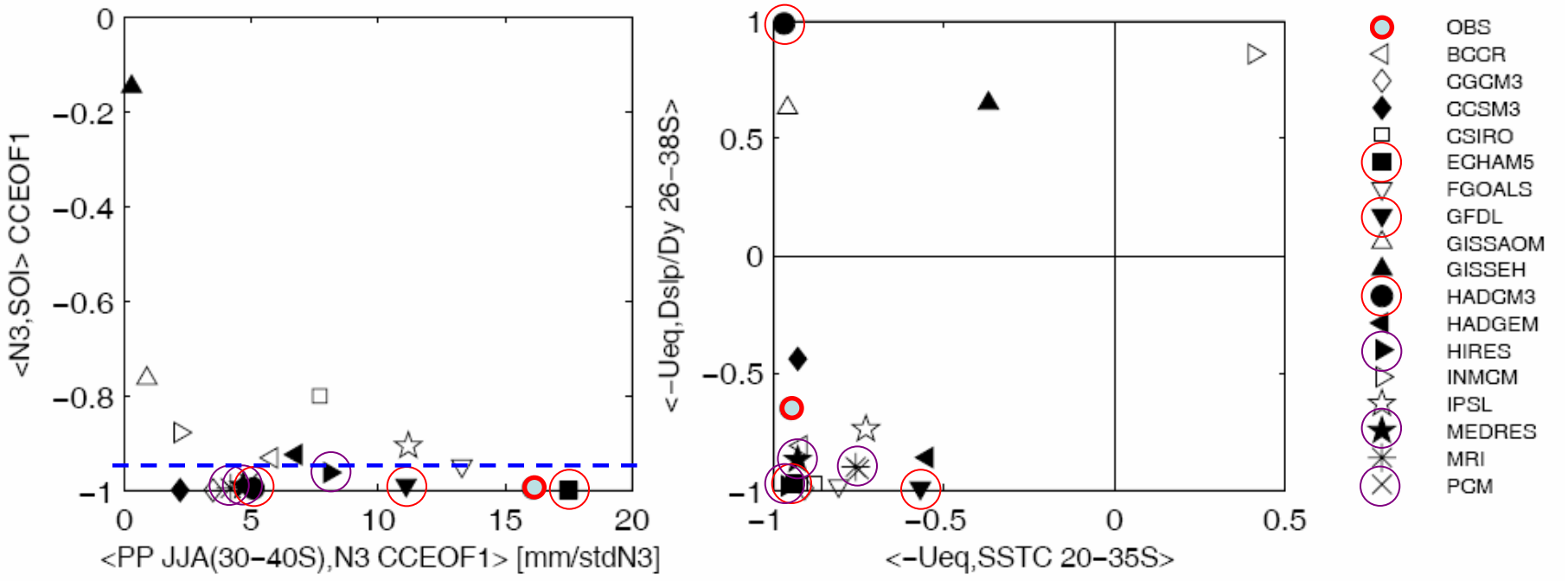

Weaker easterlies
Positive SST anomalies

Weaker easterlies
Weaker coastal jet

Conclusion…

ECHAM5/MPI-OM is the model for our region…

Reconstructed Niño 3 SST from the first SST-SLP combined complex empirical orthogonal function (CCEOF1) mode in the South Pacific Ocean – ENSO-like TIMESCALE

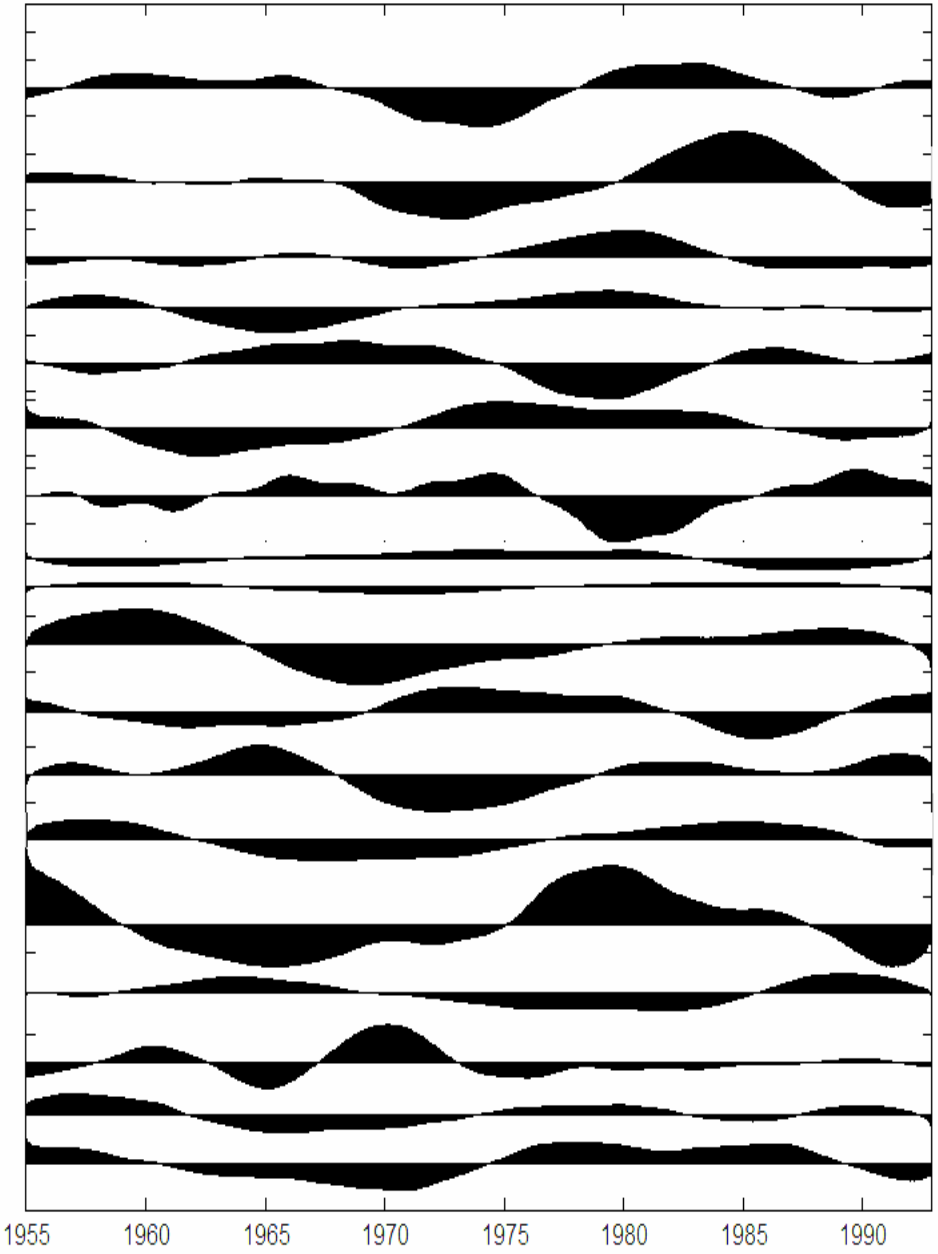

	σ_{N3}	σ_{SOI}	$r_{N3.SOI}$	$\%_{modo1}$
OBS	0,12	0,35	-0,98	55
BCCR	0,16	0,03	-0,99	48
CGCM3	0,08	0,10	-0,99	46
CCSM3	0,08	0,08	-0,75	45
CSIRO	0,12	0,15	-0,94	50
ECHAM5	0,12	0,06	-0,98	57
FGOALS	0,13	0,12	-0,88	43
GFDL	0,05	0,06	-0,52	42
GISSAOM	0,03	0,02	0,27	49
GISSEH	0,15	0,06	-0,42	67
HADCM3	0,09	0,14	-0,90	57
HADGEM	0,12	0,30	-0,96	53
HIRES	0,10	0,08	~ -1	57
INMCM	0,22	0,11	-0,59	56
IPSL	0,08	0,07	-0,04	51
MEDRES	0,10	0,14	-0,93	48
MRI	0,08	0,11	-0,96	50
PCM	0,11	0,10	-0,78	51

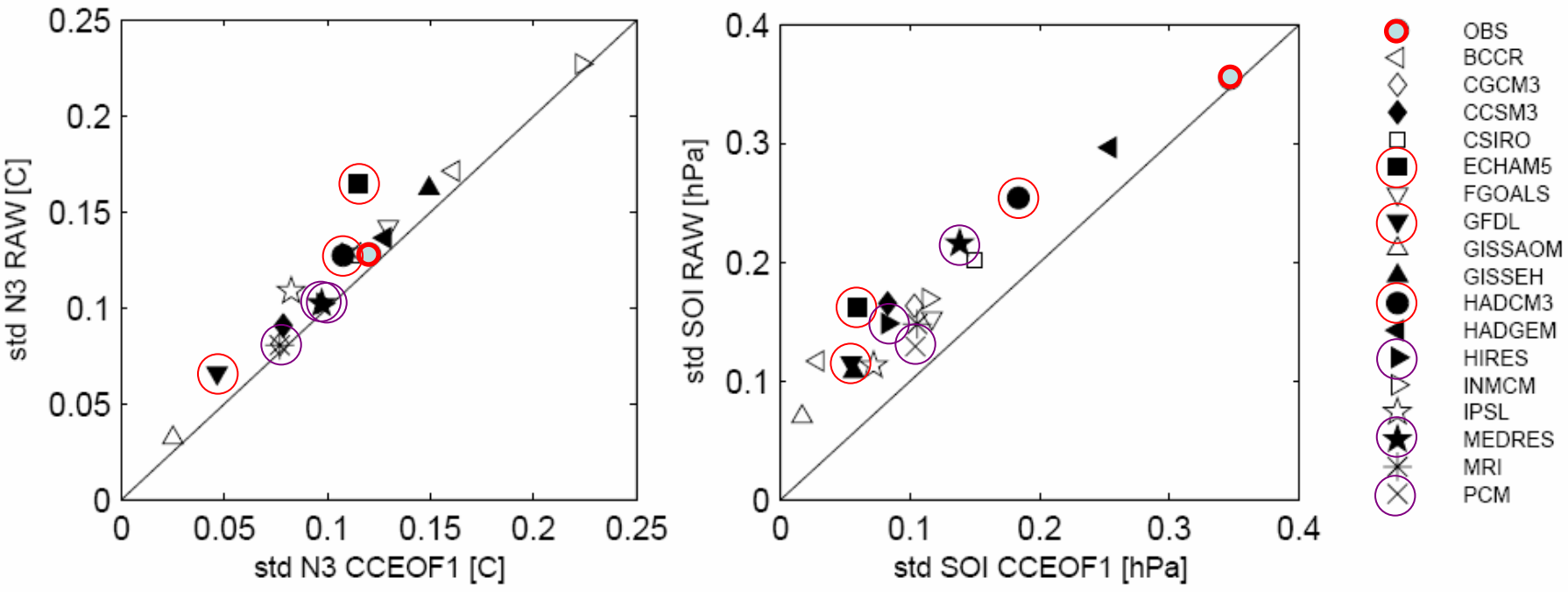
std N3 RAW [C]
std N3 CCEOF1 [C]
0
0.05
0.1
0.15
0.2
0.25
std SOI RAW [hPa]
std SOI CCEOF1 [hPa]
0.3
0.4
OBS
BCCR
CGCM3
CCSM3
CSIRO
ECHAM5
FGOALS
GFDL
GISSAOM
GISSEH
HADCM3
HADGEM
HIRES
INMCM
IPSL
MEDRES
MRI
PCM

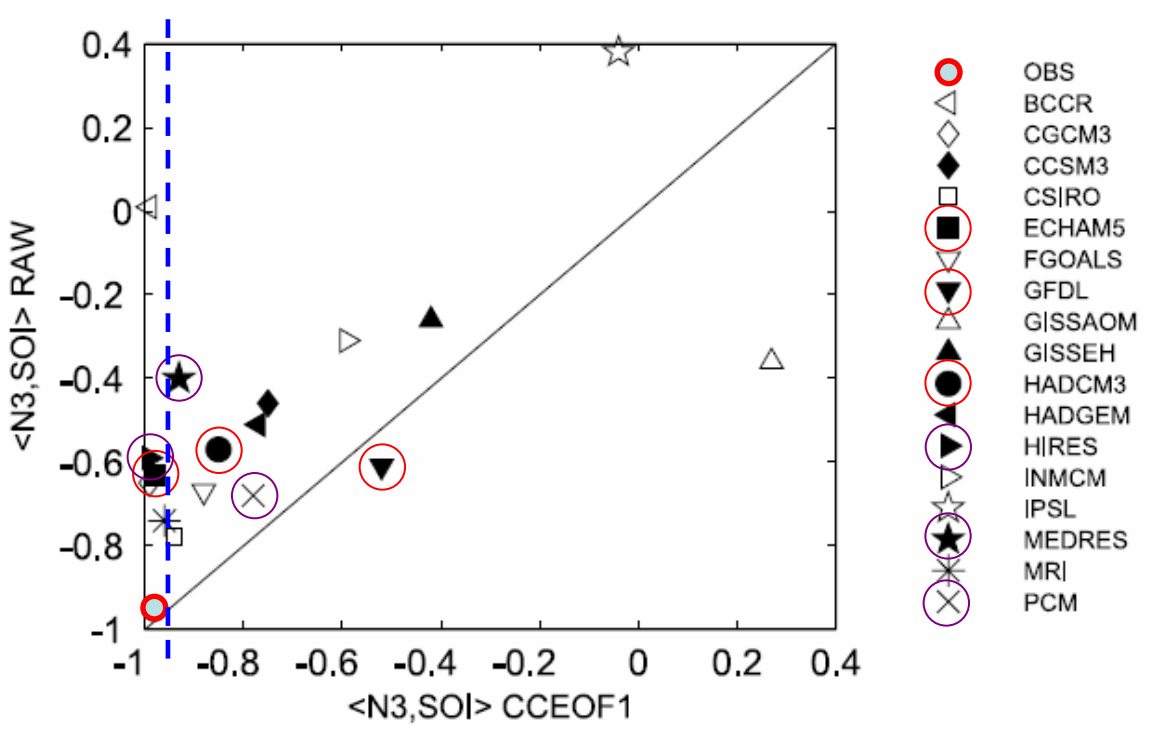
0.4
0.2
0
-0.2
-0.4
-0.6
-0.8
-1
-1
-0.8
-0.6
-0.4
-0.2
0
0.2
0.4
<N3,SOI> RAW
<N3,SOI> CCEOF1
OBS
BCCR
CGCM3
CCSM3
CS|RO
ECHAM5
FGOALS
GFDL
G|SSAOM
GISSEH
HADCM3
HADGEM
H|RES
INMCM
IPSL
MEDRES
MR|
PCM

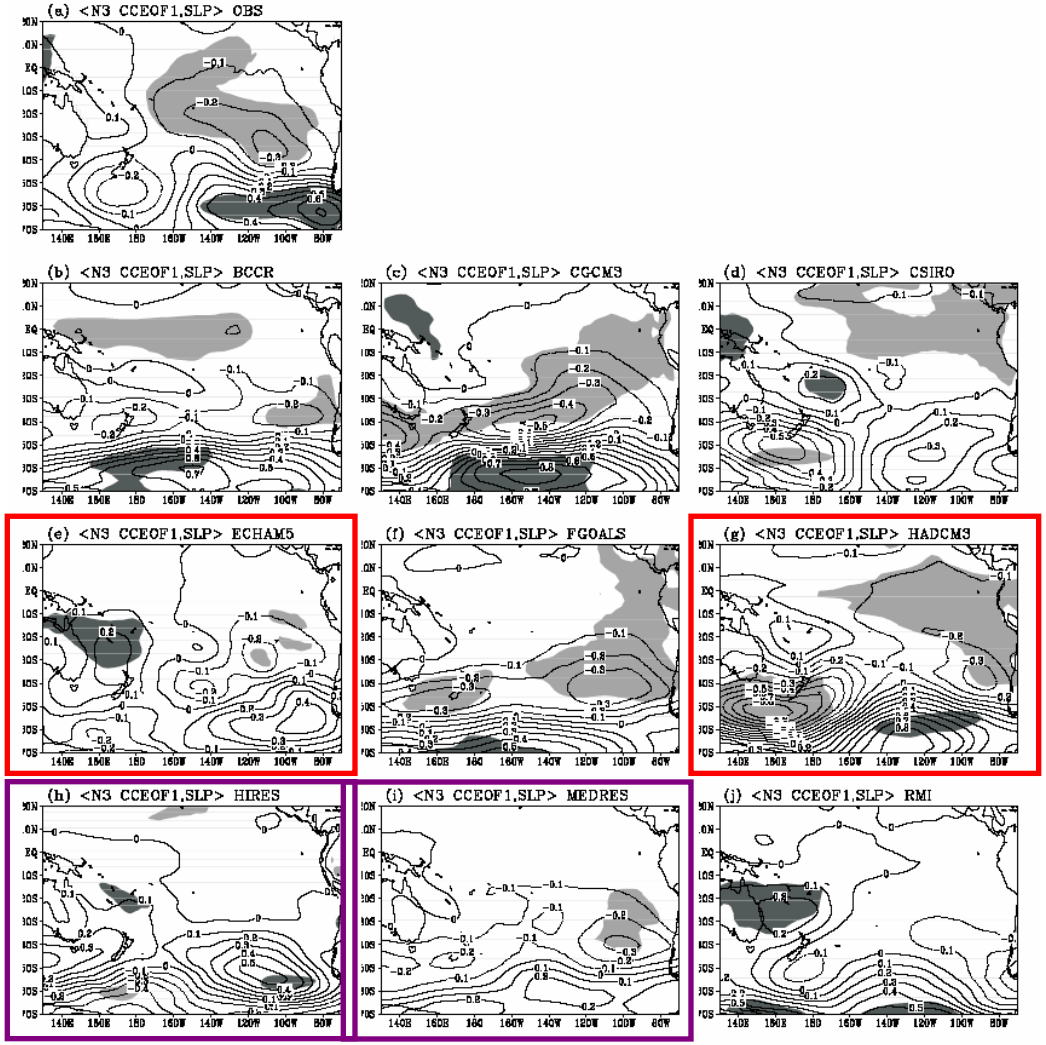

Figure 4. Reconstructed CCEOF1 Niño 3 SST Index (N3; see Figure 1) regressed upon raw SLP anomaly field using observed and simulated SST and SLP interdecadal anomalies. Positive (solid line) and negative (dashed line) regression coefficients are depicted every 0.1 hPa per N3 standard deviation, and the dark (light) shaded areas depict correlation coefficients larger (lower) than 0.7 (-0.7). The zero line is not shown. The |0.7| correlation coefficient represents approximately the 95% of confidence limit, applying the random-phase test of *Ebisuzaki* [1997].

Conclusions

- **Most models are unable to reproduce the main (basic) SST-SLP coupled relationship in the tropical Pacific, at interannual and interdecadal timescales (Bjerknes' mechanism).**

- **Unlike SST, simulated SLP anomalies are weaker than observed.**

- **Some of them, however, are capable to reproduce important characteristics of ENSO related climate anomalies in Chile: teleconnection patterns and impact on rainfall, coastal SST and surface air temperature.**

- **ECHAM5/MPI-OM is the model…**

Main SST-SLP coupled modes in the South Pacific as simulated by IPCC-AR4 coupled models

Aldo Montecinos
Departamento de Geofísica
Universidad de Concepción

II Simposio Internacional de Climatología, Sao Pablo, Brasil, 2-3 noviembre 2007

DGEO
Universidad de Concepción